

1 Zeppelin-led study on the onset of new particle formation in the planetary boundary layer

2

3 Janne Lampilahti¹, Hanna E. Manninen², Tuomo Nieminen¹, Sander Mirme³, Mikael Ehn¹, Iida
4 Pullinen⁴, Katri Leino¹, Siegfried Schobesberger^{1,4}, Juha Kangasluoma¹, Jenni Kontkanen¹, Emma
5 Järvinen⁵, Riikka Väänänen¹, Taina Yli-Juuti⁴, Radovan Krejci⁶, Katrianne Lehtipalo^{1,7}, Janne
6 Levula¹, Aadu Mirme³, Stefano Decesari⁸, Ralf Tillmann⁹, Douglas R. Worsnop^{1,4,10}, Franz Rohrer⁹,
7 Astrid Kiendler-Scharr⁹, Tuukka Petäjä^{1,11}, Veli-Matti Kerminen¹, Thomas F. Mentel⁹, and Markku
8 Kulmala^{1,11,12}

9

10 ¹Institute for Atmospheric and Earth System Research / Physics, Faculty of Science, University of
11 Helsinki, Helsinki, Finland.

12 ²CERN, CH-1211 Geneva, Switzerland.

13 ³Institute of Physics, University of Tartu, Tartu, Estonia.

14 ⁴Department of Applied Physics, University of Eastern Finland, Kuopio, Finland.

15 ⁵National Center for Atmospheric Research, Boulder, CO, USA.

16 ⁶Department of Environmental Science & Bolin Centre for Climate research, Stockholm University,
17 Stockholm, Sweden.

18 ⁷Finnish Meteorological Institute, Helsinki, Finland.

19 ⁸Istituto di Scienze dell'Atmosfera e del Clima, CNR, Bologna, Italy.

20 ⁹Institute for Energy and Climate Research, IEK-8, Forschungszentrum Jülich GmbH, Jülich,
21 Germany.

22 ¹⁰Aerodyne Research Inc, Billerica, MA, USA.

23 ¹¹Joint International Research Laboratory of Atmospheric and Earth System Sciences, Nanjing
24 University, Nanjing, China.

25 ¹²Aerosol and Haze Laboratory, Beijing Advanced Innovation Center for Soft Matter Science and
26 Engineering, Beijing University of Chemical Technology, Beijing, China.

27

28 Correspondence to: Janne Lampilahti (janne.lampilahti@helsinki.fi)

29

30 **Abstract**

31 We compared observations of aerosol particle formation and growth in different parts of the
32 planetary boundary layer at two different environments that have frequent new particle formation
33 (NPF) events. In summer 2012 we had a campaign in Po Valley, Italy (urban background) and in
34 spring 2013 a similar campaign took place in Hyytiälä, Finland (rural background). Our study

35 | consists of three case studies of airborne and ground-based measurements of ion and particle size
36 | distribution from ~ 1 nm. The airborne measurements were performed using a Zeppelin inside the
37 | boundary layer up to 1000 m altitude. Our observations show the onset of regional NPF and the
38 | subsequent growth of the aerosol particles happening almost uniformly inside the mixed layer (ML)
39 | in both locations. However, in Hyytiälä we noticed local enhancement in the intensity of NPF
40 | caused by mesoscale BL dynamics. Additionally, our observations indicate that in Hyytiälä NPF
41 | was probably also taking place above the ML. In Po Valley we observed NPF that was limited to a
42 | specific air mass.

43 |

44 | **1 Introduction**

45 | The boundary layer (BL) is the lowest layer of the earth's atmosphere (Stull, 1988). The BL is an
46 | interface controlling the exchange of mass and energy between atmosphere and surface. Ground
47 | based measurements are often used as representative observations for the whole BL. However they
48 | cannot cover vertical internal variability of BL and this can be addressed only by airborne
49 | observations.

50 |

51 | Figure 1 show the typical BL evolution over land during the time span on one day. Shortly after
52 | sunrise convective mixing creates a mixed layer (ML) that rapidly grows during the morning by
53 | entraining air from above and can reach an altitude of $\sim 1-2$ km above the surface. The ML is capped
54 | by a stable layer at the top. Above the BL is the free troposphere (FT), which is decoupled from the
55 | surface. Here we define BL to mean all the layers below the FT. Around sunset convective mixing
56 | and turbulence diminishes and the ML becomes what is known as the residual layer (RL). During
57 | the night a stable boundary layer develops due to interaction with the ground surface. This layer has
58 | only weak intermittent turbulence and it smoothly blends into the RL.

59 | The boundary layer (BL) is the lowest layer of the earth's atmosphere (Stull, 1988). The BL is an
60 | interface controlling the exchange of mass and energy between atmosphere and surface. Ground
61 | based measurements are often used as representative observations for the whole BL. However they
62 | cannot cover vertical internal variability of BL and this can be addressed only by airborne
63 | observations.

64 |

65 | Figure 1 show the typical BL evolution over land during the time span on one day. Shortly after
66 | sunrise convective mixing creates a mixed layer (ML) that rapidly grows during the morning by
67 | entraining air from above and can reach an altitude of $\sim 1-2$ km above the surface. The ML is capped
68 | by a stable layer at the top. Above the BL is the free troposphere (FT), which is decoupled from the

69 ~~surface. Here we define BL to mean all the layers below the FT. Around sunset convective mixing~~
70 ~~and turbulence diminishes and the ML becomes what is known as the residual layer (RL). During~~
71 ~~the night a stable boundary layer develops due to interaction with the ground surface. This layer has~~
72 ~~only weak intermittent turbulence and it smoothly blends into the RL.~~

73 |
74 We studied where new particle formation (NPF) occurs in the BL and how it relates to BL
75 evolution, comparing two different environments. NPF refers to the formation of nanometer sized
76 clusters from low-volatility vapors present in the atmosphere, and their subsequent growth to larger
77 aerosol particles (Kulmala et al., 2013). Understanding NPF better is of major interest, since it is a
78 dominant source of cloud condensation nuclei in the atmosphere and therefore can have important
79 indirect effects on climate (Dunne et al., 2016; Gordon et al., 2017; Pierce and Adams, 2009; Yu and
80 Luo, 2009).

81
82 Nilsson et al. (2001) studied NPF in a boreal forest environment and observed that in addition to
83 increased solar radiation the onset of turbulence appears to be a necessary trigger for NPF. Several
84 explanations for this connection were proposed: NPF might be starting in the RL or at the top of the
85 shallow ML, from where the aerosol particles are mixed to the surface as the ML starts to grow.
86 NPF starts in the ML due to dilution of pre-existing aerosol and drop in vapor sink. Convective
87 mixing brings different precursor gases, one present in the RL and the other in the ML, into contact
88 with each other initiating NPF inside the ML.

89 |
90 Airborne measurements of nanoparticles from different environments show that NPF occurs in
91 many parts of the BL. Multiple observations from Central Europe suggest that aerosol particles are
92 formed on top of a shallow ML (Platis et al., 2015; Siebert et al., 2004; Chen et al., 2018) or inside
93 the RL (Stratmann et al., 2003; Wehner et al., 2010). Other results come from a boreal forest
94 environment in southern Finland. Lampilahti et al. (2021) showed evidence that NPF may occur in
95 the interface between the RL and the FT. O'Dowd et al. (2009) observed the first signs of NPF in
96 the surface ML and Leino et al. (2019) showed that sub-3 nm particles have higher concentration
97 close to surface. Laakso et al. (2007) performed hot-air balloon measurements and concluded that
98 NPF either took place throughout the ML or in the lower part of the ML. Measurements by
99 Schobesberger et al. (2013) suggested that NPF was more intense in the top parts of a developed
100 ML. More measurements are needed in order to understand these mixed results.

101 ~~Nilsson et al. (2001) studied NPF in a boreal forest environment and observed that in addition to~~
102 ~~increased solar radiation the onset of turbulence appears to be a necessary trigger for NPF. Several~~

103 explanations for this connection were proposed: NPF might be starting in the RL or at the top of the
104 shallow ML, from where the aerosol particles are mixed to the surface as the ML starts to grow.
105 NPF starts in the ML due to dilution of pre-existing aerosol and drop in vapor sink. Convective
106 mixing brings different precursor gases, one present in the RL and the other in the ML, into contact
107 with each other initiating NPF inside the ML.

108
109 Airborne measurements of nanoparticles from different environments show that NPF occurs in
110 many parts of the BL. Multiple observations from Central Europe suggest that aerosol particles are
111 formed on top of a shallow ML (Platis et al., 2015; Siebert et al., 2004; Chen et al., 2018) or inside
112 the RL (Stratmann et al., 2003; Wehner et al., 2010). Other results come from a boreal forest
113 environment in southern Finland. Lampilahti et al. (2020a) showed evidence that NPF may occur in
114 the interface between the RL and the FT. O'Dowd et al. (2009) observed the first signs of NPF in
115 the surface ML and Leino et al. (2019) showed that sub-3 nm particles have higher concentration
116 close to surface. Laakso et al. (2007) performed hot-air balloon measurements and concluded that
117 NPF either took place throughout the ML or in the lower part of the ML. Measurements by
118 Schobesberger et al. (2013) suggested that NPF was more intense in the top parts of a developed
119 ML. More measurements are needed in order to understand these mixed results.

120
121 Here we present NPF measurements on board a Zeppelin airship carried out during the EU
122 supported PEGASOS (Pan-European Gas-AeroSOls Climate Interaction Study) project. ~~The main~~
123 ~~goal of the project was to quantify the magnitude of regional to global feedbacks between~~
124 ~~atmospheric chemistry and physics, and thus quantify their impact on the changing climate.~~ The
125 Zeppelin flights were used to observe radicals, trace gases, and aerosol particles inside the lower
126 troposphere over Europe in several locations during 2012-2013.

127
128 By using a Zeppelin NT (Neue Technologie) airship we were able to sample ~~from a stable, agile~~
129 ~~platform,~~ up to 1000 meters above sea level (asl). The high payload capacity of the Zeppelin
130 enabled us to carry state-of-the-art instrumentation, specifically designed to collect
131 information on the feedback processes between the chemical compounds and the smallest
132 aerosol particles to better estimate their role in climate and air quality.

133
134 The NPF focused campaigns presented here were performed in Po Valley, Italy, and Hyytiälä,
135 Finland. At both locations NPF events happen frequently. Po Valley represents urban background
136 conditions where anthropogenic emissions are an important source of gaseous precursors for NPF

137 (e.g. Kontkanen et al., 2016). Hyytiälä represents rural background conditions where organic vapors
138 from the surrounding forests play a major role in NPF (e.g. Dada et al., 2017).

139

140 Here we combine comprehensive ground-based and airborne measurements [from the Zeppelin](#) to
141 [investigate](#) ~~compare~~ two NPF cases from Po Valley ~~and to~~ one case from Hyytiälä. The Zeppelin
142 allowed us to repeatedly profile the lowest 1 km of the atmosphere providing a full picture of what
143 is happening in the BL during the onset of NPF. We will show in which part or parts of the BL the
144 onset of NPF and the subsequent particle growth occurred at the two measurement sites as well as
145 determine formation and growth rates for the aerosol particles.

146

147 **2 Methods**

148 [The two ground-based measurement sites that were studied here were](#) San Pietro Capofiume in
149 Po Valley, Italy and Hyytiälä in Southern Finland ~~are interesting environments to compare~~
150 ~~from nucleation and particle growth point of view because NPF is frequently observed in~~
151 ~~both environments~~. The vertical measurement profiles analyzed in this study were
152 performed in a close proximity to the ground-based measurement sites.

153

154 **2.1 San Pietro Capofiume, Italy**

155 San Pietro Capofiume (SPC, 44°39'N 11°37'E, 11 m asl) is located in the eastern part of Po Valley,
156 Italy, between the cities of Bologna and Ferrara. Po Valley is considered a pollution hot spot,
157 although, the station itself is surrounded by vast agricultural fields away from point sources. Thus
158 the aerosol concentration and composition at SPC reflect the Po Valley regional background. NPF is
159 frequently observed in SPC (36% of days) with maxima in May and July (Hamed et al., 2007;
160 Laaksonen et al., 2005).

161

162 The instruments measuring the aerosol particle number-size distribution were a scanning mobility
163 particle sizer (SMPS, 10-700 nm, 5 min time resolution; Wiedensohler et al., 2012) and a neutral
164 cluster and air ion spectrometer (NAIS, particles: ~2-40 nm, ions: 0.8-40 nm, 4 min time resolution;
165 Mirme and Mirme, 2013). We used the NAIS's positive polarity for the particle number size
166 distribution data. The ML height was determined from ceilometer (Lufft CHM 15k) measurements.
167 Basic meteorology and SO₂ gas concentration data (Thermo 43iTLE monitor) were also available at
168 surface level (2-3 m above ground level).

169

170 **2.2 Hyytiälä, Finland**

171 In Finland the ground-based measurements were performed at the SMEAR II (Station for
172 Measuring Forest Ecosystem-Atmosphere Relations II) station located in Hyytiälä, Finland (HTL,
173 61°51'N 24°17'E, 181 m asl; Hari and Kulmala, 2005). The station is equipped with extensive
174 facilities to measure the forest ecosystem and the atmosphere. The measurement site is surrounded
175 by coniferous boreal forest.

176

177 The forest emits biogenic volatile organic compounds (Hakola et al., 2003), which can be oxidized
178 in the atmosphere to form low-volatile vapors that contribute to aerosol particle formation and
179 growth (Ehn et al., 2014; Mohr et al., 2019). NPF is frequently observed in HTL (23% of all days),
180 especially in spring and autumn (Dal Maso et al., 2005; Nieminen et al., 2014).

181 Aerosol particle and ion number-size distributions were measured by the station's differential
182 mobility particle sizer (DMPS, 3-1000 nm, 10 min time resolution; Aalto et al., 2001) and the NAIS
183 (Manninen et al., 2009). Sub-3 nm particle number-size distribution was measured by a particle size
184 magnifier running in scanning mode (PSM, 1.2-2.5 nm, 10 min time resolution; Vanhanen et al.,
185 2011). Also a PSM measured at SPC but we were not able to reliably calculate formation rates from
186 the data. Basic meteorological variables, radiation, and SO₂ were measured from the station's mast
187 at 16.8 meters above ground. In addition, a supporting NPF forecast tool was developed to aid the
188 planning of research flights (Nieminen et al., 2015).

189

190 **2.3 Zeppelin NT airship**

191 A Zeppelin NT airship was used for monitoring the atmosphere below 1 km. The aerosol particles
192 and trace gases were sampled with instrumentation installed inside the Zeppelin's cabin. The
193 Zeppelin operated with three different instrument layouts. A specific layout was chosen according to
194 the flight plan and scientific aim of the flight.

195

196 Here we analyzed data from measurement flights that carried the so-called nucleation layout.
197 Instruments specific to this layout were the atmospheric pressure interface time-of-flight mass
198 spectrometer (APi-TOF; Junninen et al., 2010), used for measuring the elemental composition of
199 naturally charged ions and the NAIS for particle and ion number size distributions. We also used the
200 aerosol number-size distribution data from the SMPS (10-400 nm, 4 min time resolution) and PSM
201 running in scanning mode, which were on board during all the measurement flights. The size range
202 and time resolution of the onboard NAIS and PSM were same as for the instruments in HTL (see
203 Section 2.1).

204

205 During a measurement flight the Zeppelin did multiple vertical profiles over a small area ($\sim 10 \text{ km}^2$).
206 The profiling spot was picked typically down-wind from the measurement site in order not to
207 compromise the ground-based measurements with any emissions. The vertical extent of the profiles
208 was $\sim 100\text{-}1000 \text{ m}$ above the ground. The airspeed during measurement was $\sim 20 \text{ m/s}$ and the
209 vertical speed during ascend and descend was $\sim 0.5 \text{ m/s}$ and $\sim 3 \text{ m/s}$ respectively.

210

211 | **2.4. Cessna 172 airplane**

212 | During the PEGASOS northern mission in spring 2013, a Cessna 172 airplane carrying scientific
213 instrumentation was deployed to measure aerosol particles, trace gases and meteorological variables
214 in the lower troposphere alongside the Zeppelin. The measurement setup and instrumentation on
215 board have been described in previous studies (Lampilahti et al., 2020b; Schobesberger et al., 2013;
216 Leino et al., 2019; Väänänen et al., 2016)

217 | **2.4. Cessna 172 airplane**

218 | During the PEGASOS northern mission in spring 2013, a Cessna 172 airplane carrying scientific
219 instrumentation was deployed to measure aerosol particles, trace gases and meteorological variables
220 in the lower troposphere alongside the Zeppelin. The measurement setup and instrumentation on
221 board have been described in previous studies (Schobesberger et al., 2013; Lampilahti et al., 2020c;
222 Leino et al., 2019; Väänänen et al., 2016).

223 |

224 Basic meteorological variables (temperature, pressure, relative humidity) were measured on board.
225 Particle number-size distribution was measured using a SMPS (10-400 nm size range, 2 min time
226 resolution) and the number concentration of $>3 \text{ nm}$ particles was measured using an ultrafine
227 condensation particle counter (UF-CPC, TSI model 3776) at 1 s time resolution. The altitude range
228 of the airplane was $\sim 100\text{-}3000 \text{ m}$ above ground and the measurement airspeed was 36 m/s .

229

230 | **2.5 Flight profiles and atmospheric conditions**

231 | Our measurements focused on the time of BL development from sunrise until noon (Figure 14).

232 | This is the time when the onset of NPF is typically observed at the ground level. The vertical
233 | profile measurements represent the particle and gas concentrations in the lower parts of the
234 | atmosphere: the mixed layer, the residual layer, the nocturnal boundary layer. At the same
235 | time, the ground-based measurements recorded conditions in the surface layer. Here we
236 | consider the BL to include all the atmospheric layers below the free troposphere.

237

238 The basic conditions for the Zeppelin flights in both Italy and Finland were clear sky and low wind
239 speed. Under these conditions, the sun heats the surface during the morning, which drives intense
240 vertical mixing.

241

242 **2.6 Data analysis**

243 The onset of NPF occurs when low-volatility vapors in the atmosphere form nanometer sized
244 clusters that continue to grow to larger aerosol particles (Kulmala et al., 2013).

245

246 We determined the onset of a NPF event visually from the initial increase in the number
247 concentration of intermediate (2-4 nm) air ions at the beginning of the NPF event. An increase in
248 the intermediate ion concentration has been identified as a good indicator for NPF (Leino et al.,
249 2016). This is because an increase in the number concentration of intermediate ions is usually due
250 to NPF and otherwise the number concentration is extremely low (below 5 cm^{-3}).

251

252 Particle growth rates (GR), formation rates and coagulation sinks were calculated in different size
253 ranges according to the methods described by Kulmala et al. (2012). For particles and ions in the 1-
254 2 nm and 2-3 nm size range the GR was determined from the ion number-size distribution measured
255 by the NAIS. During NPF the number concentration in each size channel increased sequentially as
256 the freshly formed particles grew larger. We determined the time when the number concentration
257 began to rise in each size bin by fitting a sigmoid function to the rising concentration edge and
258 finding the point where the sigmoid reached 75% of its maximum value (appearance time method;
259 Lehtipalo et al., 2014). The corresponding diameter in each size bin was the bin's geometric mean
260 diameter. Before the fitting procedure the number concentrations were averaged using a 15 min
261 median and after that divided by the maximum concentration value in each size channel.

262

263 For larger particles and ions (3-7 nm and 7-20 nm) the GR was determined by fitting a log-normal
264 distribution over the growing nucleation mode at each time step and assigning the fitted curve's
265 peak value as the corresponding mode diameter. In each size range a value for the GR was obtained
266 as the slope of a linear least squares fit to the time-diameter value pairs.

267

268 The formation rate of 1.5 nm particles and ions was determined from the PSM data and the NAIS
269 ion data respectively (Kulmala et al., 2012). The formation rate of 3 nm particles and ions was
270 determined from the NAIS data. Coagulation sinks were calculated from the SMPS or DMPS data.
271 Condensation sink for sulfuric acid was calculated from the Zeppelin's on board SMPS.

272

273 Sulfuric acid (SA) is a key compound in atmospheric nucleation (Sipilä et al., 2010). As we did not
274 have direct measurements of SA concentration, we used [HSO₄⁻] from the API-TOF measurements
275 as a qualitative indicator of [H₂SO₄] and named it pseudo-SA. To determine this pseudo-SA, we
276 summed up all ions containing HSO₄⁻, e.g. the ion itself but also larger clusters, like
277 (H₂SO₄)_n*HSO₄⁻. We assumed steady state conditions and that the concentration of SA-containing
278 ions is much lower than the total ion concentration. Under these conditions [HSO₄⁻] (including all
279 clusters where this ion was present) can be considered close to a linear function of [H₂SO₄] (Eisele
280 and Tanner, 1991). At the highest SA loadings, ions with HSO₄⁻ can be a dominant fraction of the
281 total ions (Ehn et al., 2010), in which case the linearity no longer holds. In addition, this assumes a
282 constant concentration of ions, although for example the sinks for ions can vary, e.g. by an
283 increased particle concentration. As such, the pseudo-SA parameter should indeed only be
284 considered a qualitative indicator for SA.

285

286 In SPC the ML height was derived from the ceilometer measurements. However, in HTL weak
287 scattering signal prevented reliable determination of ML height using the on-site lidar. For this
288 reason in HTL the ML height was determined from vertical profiles of meteorological variables and
289 aerosol particle concentrations on board the Zeppelin and the Cessna 172 airplane. In these profiles
290 the top of the ML was revealed by the maximum positive gradient in potential temperature and
291 minimum negative gradient in humidity and total particle number concentration (Stull, 1988).

292

293 The origin of the air masses was investigated using back trajectory analysis. The trajectories were
294 calculated with the HYSPLIT (Hybrid Single Particle Lagrangian Integrated Trajectory; Stein et al.,
295 2015) model using the GDAS (Global Data Assimilation System) archived data sets.

296

297

298 **3 Results and discussion**

299

300 **3.1 Case study description**

301

302 During the campaigns there were a limited number of flights with the nucleation instrument payload
303 (Po Valley: 19.6.2012, 27.6.2012 , 28.6.2012 , 29. 6.2012 and 30.6.2012; Hyytiälä: 6.5.2013,
304 8.5.2013, 16.5.2013, 3.6.2013, 8.6.2013 and 10.6.2013). Here we present a side by side comparison
305 of two case studies, one from SPC (June 28, 2012) and the other from HTL (May 8, 2013). On these

306 | days the NPF event was fully captured during the Zeppelin measurement. In addition the horizontal
307 | extent of NPF in SPC was investigated by studying the measurement flight from June 30, 2012.

308 |

309 | **3.1 Case study description**

310 | ~~During the campaigns there were a limited number of flights with the nucleation instrument~~
311 | ~~payload. Here we present a side-by-side comparison of two case studies, one from SPC (June 28,~~
312 | ~~2012) and the other from HTL (May 8, 2013). In addition the horizontal extent of NPF in SPC was~~
313 | ~~investigated by studying the research flight from June 30, 2012.~~

314 |

315 | June 28, 2012 was a hot and sunny day in Po Valley. 24-h back trajectories arriving to SPC during
316 | the morning revealed that the incoming air masses circulated from Central Europe and over the
317 | Adriatic Sea before arriving to SPC from the southwest (Figure 22a). Figure 33 shows the time
318 | series for some environmental parameters on the NPF event days from SPC and HTL. In SPC
319 | temperature and RH showed a large diurnal variation; the temperature increased from 16 °C to 32
320 | °C during the morning while the RH decreased from 87% to 39%. The mean wind speed at 10 m
321 | height was 2.0 m s⁻¹. These meteorological conditions and air mass histories are common during
322 | NPF event days in Po Valley (Hamed et al., 2007; Sogacheva et al., 2007).

323 |

324 | May 8, 2013 in HTL was a sunny and warm day with clear skies marked by broad diurnal
325 | variation in temperature and RH. During the morning the temperature increased from 5 °C
326 | to 17 °C and the RH decreased from 82% to 25%. The mean wind speed at 33.6 m height
327 | was 3.5 m s⁻¹. The air masses originated from the North Atlantic Ocean arriving to HTL
328 | from the northwest via Scandinavia and the Gulf of Bothnia (Figure 22b). Most NPF event
329 | days in HTL are clear sky days with the arriving air masses spending most of their time in
330 | the northwest sector (Dada et al., 2017; Nilsson et al., 2001; Sogacheva et al., 2008).

331 |

332 | In SPC the solar radiation began to increase after 04:00 and according to the ceilometer
333 | measurements the ML started to increase in height around 06:00, at the same time the SO₂
334 | concentration and N_{>10} (number concentration of particles larger than 10 nm) began to increase.
335 | This is likely explained by the entrainment of pollutants from the RL and the onset of NPF. CS is
336 | higher during the night and decreases slightly during the day, which is likely due to dilution related
337 | to ML growth.

338 |

339 At HTL after sunrise the SO₂ concentration and N_{>10} decreased probably due to the dilution caused
340 by the growing ML coupled with the lack of pollution sources. While SO₂ concentration remained
341 low the whole day, N_{>10} and CS began to increase later during the day because of the NPF event.
342 The average SO₂, N_{>10} and CS in SPC were 0.57 ppb, 8102 cm⁻³ and 0.0128 s⁻¹ respectively. While
343 in HTL the corresponding values were 0.02 ppb, 3293 cm⁻³ and 0.0007 s⁻¹.

344

345 3.2 Onset of NPF

346 | Figures 44a and 44b show the altitude of the Zeppelin as a function of time colored by the number
347 concentration of intermediate ions measured by the NAIS at SPC and HTL. The plots also show the
348 number concentration of intermediate ions measured on the ground as well as the ML height.

349

350 In SPC, the intermediate ion concentration began to increase on the ground at 5:48, which coincides
351 with the beginning of convective mixing and the breakup of the nocturnal surface layer. Similarly,
352 Kontkanen et al. (2016) observed that in Po Valley the onset of NPF coincided with the beginning
353 of boundary layer growth. Around this time the Zeppelin was profiling the layers above the ML.
354 “Pockets” of elevated intermediate ion concentration were present inside the RL (for example
355 around 700 m at 5:15). These pockets were not linked to the NPF event inside the ML. When the
356 Zeppelin later entered the ML at around 6:45, NPF was already taking place throughout the
357 developing ML and seemed to be confined to it.

358

359 In HTL, the number concentration of intermediate ions began to increase at around 6:47 on the
360 ground level. The ML at this point had grown to around 600 m above ground, which
361 allowed us to better resolve the onset of NPF vertically. In HTL no increase in intermediate
362 | ion concentration, indicating no NPF, was observed above the ML on board the Zeppelin.
363 Before 6:40 there was no sign of NPF inside the growing ML. Between 6:40 and 7:00 the
364 Zeppelin briefly measured in the RL and re-entered the ML at 7:00. At this point the
365 intermediate ion concentration was already increasing on board similar to the ground level,
366 indicating the onset of NPF.

367

368 | Figure 55 shows the intermediate ion number concentration as a function of time from the
369 Zeppelin and the SMEAR II station. At the beginning of the NPF event, between 07:00-
370 07:15, the Zeppelin ascended from 300 m to 800 m. During the ascend the intermediate ion
371 concentrations increased at a similar rate and stayed at similar values on board the Zeppelin
372 and at the ground level. The lack of vertical gradient in the number concentration suggests

373 that the aerosol particles were forming homogeneously throughout the ML. However,
374 intense turbulent mixing and strong updrafts moving up at roughly the same rate as the
375 Zeppelin might have also resulted in a homogeneous number concentration, even if the
376 aerosol particles were formed close to the surface.

377 |
378 ~~Figures 4c and 4d show the Zeppelin's measurement profiles colored with the pseudo SA. In SPC,~~
379 ~~the highest amount of pseudo SA appears to be in the residual layer above the growing morning ML~~
380 ~~(also observed on June 27, 2012) after sunrise. This is in line with the observation that the SO₂-~~
381 ~~concentration increases at the surface when the ML starts to grow (Figure 3b), indicating that the~~
382 ~~SO₂ was entrained from the RL. The entrainment of SO₂ from the residual layer is also supported by~~
383 ~~previous observations (Kontkanen et al., 2016). The increased pseudo SA in the residual layer was~~
384 ~~not associated with NPF in the residual layer.~~

385 |
386 Figures 4c and 4d show the Zeppelin's measurement profiles colored with the pseudo SA. In SPC,
387 the highest amount of pseudo SA appears to be in the residual layer above the growing morning ML
388 (also observed on June 27, 2012) after sunrise. This is in line with the observation that the SO₂
389 concentration increases at the surface when the ML starts to grow (Figure 3b), indicating that the
390 SO₂ was entrained from the RL. The entrainment of SO₂ from the residual layer is also supported by
391 previous observations (Kontkanen et al., 2016). The increased pseudo SA in the residual layer was
392 not associated with NPF in the residual layer.

393 In SPC the night time SO₂ concentration at the surface is low likely due to deposition (Kontkanen et
394 al., 2016). However ammonia concentration can be high (>30 µg m⁻³) at the surface due to
395 agricultural activities and the concentration has been observed to peak during the night and early
396 morning (Sullivan et al., 2016). In addition oxidized VOCs are important for aerosol particle growth
397 (Ehn et al., 2014). VOCs were measured on board the Zeppelin in Po Valley in 2012 and the results
398 showed higher VOC concentrations close to ground (Jäger, 2014). This may at least partly explain
399 why we measured increased concentrations of intermediate ions in the RL but they did not appear to
400 grow to larger sizes in any significant quantities.

401 ~~In SPC the night time SO₂ concentration at the surface is low likely due to deposition (Kontkanen et~~
402 ~~al., 2016). However ammonia concentration can be high (>30 µg m⁻³) at the surface due to~~
403 ~~agricultural activities and the concentration has been observed to peak during the night and early~~
404 ~~morning (Sullivan et al., 2016).~~

405 |

406 Since in SPC the onset of NPF coincides with the beginning of ML growth, it is possible that the
407 entrainment of SA from the residual layer into the growing ML where ammonia, and likely also
408 amines from agricultural activities, are present can lead to stabilization of the SA clusters by the
409 ammonia and amines and subsequent NPF (e.g. Almeida et al., 2013; Kirkby et al., 2011).

410

411 In SPC the pseudo-SA layer closely corresponded to a layer of reduced condensation sink (CS).

412 In low CS regions more SA is in the gas phase and therefore detected by the APi-TOF
413 (Figures 44e and 44f), which probably explains why the layer is there. In addition, the CS is
414 also a sink for ions, which means that the pseudo-SA is likely decreased even more than SA,
415 assuming that the loss rate is higher for ions than for SA molecules. By contrast, in HTL the
416 amount of pseudo-SA is higher inside the ML than above it. The pseudo-SA concentration
417 increases on board throughout the morning and peaks at roughly 9:00 and decreases
418 afterwards.

419

420 In SPC pockets of intermediate ions and a layer of pseudo SA were observed in the RL, whereas at
421 HTL intermediate ion concentrations and pseudo SA remained low in the RL. This is likely related
422 to the relatively larger anthropogenic emissions in the Po Valley region compared to HTL. In
423 previous studies NPF has been observed inside the RL in Central Europe (Wehner et al., 2010) and
424 primary nanoparticles may be released into the RL from upwind pollution sources (Junkermann and
425 Hacker, 2018).

426

427 **3.2 Particle formation and growth rates**

428 Figure 6 shows the number size distributions measured by the NAIS on board the Zeppelin and on
429 the ground from SPC and HTL. The black dots are the mean mode diameters obtained by fitting a
430 log-normal distribution over the growing particle mode.

431

432 In SPC, the number size distributions measured on board and on the ground with the NAIS (Figures
433 66a and 66c) were similar when the Zeppelin was measuring inside the ML. When the Zeppelin
434 measured above the ML the number concentration decreased and the growing mode of freshly
435 formed particles was not observed. The pockets of intermediate ions in the RL did not grow to
436 larger sizes. This can be seen as sudden disappearances of the particles, for example at around 6:40,
437 7:15 and 8:00. The observations suggests that the NPF event was limited to the ML where it was
438 taking place homogeneously.

439

440 We calculated the formation and growth rates in SPC and HTL for particles and ions on board the
441 Zeppelin and on the ground. The results are summarized in Table 14. In SPC the onset of NPF
442 happened when the ML was still very shallow and the Zeppelin was not measuring significant
443 amount of time at this low altitude (this was a problem on other NPF event days from SPC as well),
444 consequently the beginning of the NPF event was not fully observed on board. Because of this we
445 were unable to reliably calculate the formation rates and the growth rate between 1-2 nm from the
446 Zeppelin data.

447

448 Kontkanen et al. (2016) obtained formation rates of $23.5 \text{ cm}^{-3} \text{ s}^{-1}$, $9.5 \text{ cm}^{-3} \text{ s}^{-1}$, $0.1 \text{ cm}^{-3} \text{ s}^{-1}$ and 0.08
449 $\text{cm}^{-3} \text{ s}^{-1}$ for 1.5 nm particles, 2 nm particles, 2 nm positive ions and 2 nm negative ions respectively
450 for the June 28, 2012 NPF event at the ground level. These values are in line with our values for the
451 same day reported in Table 1 ($J_3 = 6.8 \text{ cm}^{-3}$, $J_3^- = 0.04 \text{ cm}^{-3}$, $J_3^+ = 0.03 \text{ cm}^{-3}$). The higher formation
452 rates in SPC compared to HTL are characteristic of polluted environments (Kerminen et al., 2018).
453 The calculated GRs for the larger particle sizes as seen in Table 1 were similar on board the
454 Zeppelin (HTL: $\text{GR}_{7-20} = 2.4 \text{ nm/h}$, SPC: $\text{GR}_{7-20} = 3.0 \text{ nm/h}$) and on the ground (HTL: $\text{GR}_{7-20} = 2.1$
455 nm/h , SPC: $\text{GR}_{7-20} = 2.8 \text{ nm/h}$).

456

457 On May 8, 2013 in HTL almost the whole NPF event was captured by the Zeppelin measuring
458 inside the ML. However, in contrast to SPC the number size distributions measured on board the
459 Zeppelin (Figure 66b) and on the ground (Figure 66d) show differences, particularly in the growing
460 nucleation mode particles. At different times on board the Zeppelin when it was measuring inside
461 the ML the particle number concentration in the growing mode momentarily increased up to eight
462 fold compared to the background number concentration, suggesting an enhancement in the particle
463 formation rate. On board the Zeppelin this can be seen as concentrated "vertical stripes" in the
464 number size distribution between 08:00-10:00. On the other hand at the ground station an increase
465 of concentration of freshly formed particles was observed between 7:30-8:00. This inhomogeneity
466 is further discussed in Section 3.3.

467

468 In the ground-based NAIS data a pool of sub-6 nm particles was present during the NPF event
469 while on board the Zeppelin no such pool was observed. This can be seen most clearly between
470 10:00-11:30 when the median particle number concentration between 2-4 nm on the ground was
471 1400 cm^{-3} whereas on board the Zeppelin it was 570 cm^{-3} . Similarly Leino et al. (2019) observed
472 that the number concentration of sub-3 nm particles decreases as a function of altitude at HTL. This

473 may be linked to increased concentration of low-volatility vapors on the surface near the sources
474 compared to aloft.

475

476 Despite the differences in the ground-based and airborne number size distributions in HTL a
477 continuous, growing, nucleation mode was observed in the "background" both on the ground
478 (alongside the pool of sub-6 nm particles) and on board the Zeppelin during the NPF event. When
479 averaged over the total duration of the NPF event, the growth rates and formation rates on board the
480 Zeppelin and on the ground were similar on this day. This would indicate that the ground-based
481 measurements represent the NPF event in the whole ML quite well. However locally increased
482 number concentrations, indicating enhanced NPF, were observed inside the ML and if the
483 enhancement is not detected with the ground-based measurements we may underestimate the
484 intensity of NPF within the ML based on ground-based data alone.

485

486 **3.3 Vertical and horizontal distribution of the freshly formed particles**

487 Next we investigated how the freshly formed particles were distributed spatially in the BL. Figure
488 [6e 7](#) shows the particle number concentration between 3-10 nm measured by the NAIS and the ML
489 height from SPC as a function of time and altitude. The freshly formed particles were distributed
490 homogeneously throughout the growing ML but were not found in the RL. The 3-10 nm number
491 concentration inside the ML was $\sim 20\,000\text{ cm}^{-3}$ while in the residual layer it was only $\sim 200\text{ cm}^{-3}$. The
492 pockets of increased intermediate ion concentration, indicating NPF in the nocturnal boundary layer
493 and residual layer (Figure [44a](#)), were not observed in the 3-10 nm size range suggesting that the
494 particles did not grow to the 3-10 nm size range in any significant numbers.

495

496 At HTL the Zeppelin was measuring in the lower half of the developed ML, however the Cessna
497 profiled the entire depth of the ML all the way up to the lower parts of the free troposphere. Figure
498 [78](#) shows the vertical profile of 3-10 nm particle number concentration between 07:00-10:00 UTC
499 calculated by subtracting the total SMPS number concentration from the UF-CPC number
500 concentration on board the Cessna. Also the water vapor concentration and temperature are shown.
501 A temperature inversion, a large negative gradient in water vapor concentration and in the particle
502 number concentration indicated that the top of the ML was present between 1300-1400 m.

503

504 On average the number concentration inside the ML remained roughly constant ($N_{3-10} \sim 1000\text{ cm}^{-3}$)
505 as a function of altitude, however there was substantial variation ($\sim 200\text{-}3000\text{ cm}^{-3}$). The strongest
506 variation came from a narrow sector roughly at the center of the measurement area, which is

507 discussed below. The NPF did not extend to the RL where the number concentrations were reduced
508 to below 100 cm⁻³.

509 |
510 However at 2000 m a layer of sub-10 nm particles was observed. The 3-10 nm number
511 concentration increased from less than 100 cm⁻³ to ~400 cm⁻³. Lampilahti et al. (2021) showed
512 evidence that NPF frequently takes place in the interface between the residual layer and the free
513 troposphere, disconnected from the ML. Precursor gases may be transported to these altitudes and
514 the mixing over the interface layer could initiate nucleation.

515 ~~On average the number concentration inside the ML remained roughly constant ($N_{3-10} \sim 1000 \text{ cm}^{-3}$)~~
516 ~~as a function of altitude, however there was substantial variation ($\sim 200\text{-}3000 \text{ cm}^{-3}$). The strongest~~
517 ~~variation came from a narrow sector roughly at the center of the measurement area, which is~~
518 ~~discussed below. The NPF did not extend to the RL where the number concentrations were reduced~~
519 ~~to below 100 cm⁻³.~~

520 |
521 ~~However at 2000 m a layer of sub-10 nm particles was observed. The 3-10 nm number~~
522 ~~concentration increased from less than 100 cm⁻³ to ~400 cm⁻³. Lampilahti et al. (2020a) showed~~
523 ~~evidence that NPF frequently takes place in the interface between the residual layer and the free~~
524 ~~troposphere, disconnected from the ML. Precursor gases may be transported to these altitudes and~~
525 ~~the mixing over the interface layer could initiate nucleation.~~

526 |
527 Figure 8a shows the particle number concentration between 3-10 nm on board the Zeppelin and the
528 airplane as a function of longitude and latitude from HTL on May 8, 2013. The particle number
529 concentration was elevated right over HTL in a narrow sector perpendicular to the mean wind
530 direction. Vertically the sector extended throughout the depth of the ML. The number concentration
531 in the sector increased 2-8 fold compared to the surrounding background number concentration. The
532 mean wind speed in the ML was about 4 m/s and the particle sector was observed throughout the
533 whole measurement flight, for at least 2.5 hours. This suggests that the particle sector was probably
534 at least 35 km long along the mean wind direction.

535 |
536 The concentrated vertical stripes over the growing nucleation mode in Figure 6b were caused by the
537 Zeppelin periodically flying through the particle sector. The sector slowly moved perpendicular to
538 the mean wind towards northeast and when passing over HTL it was seen as the plume of particles
539 in Figure 6d between 07:30-08:00. The particles in the sector grew at approximately the same rate
540 with the background NPF event particles, which also suggests that the particles were formed

541 simultaneously inside the long and narrow sector. Lampilahti et al. (2020b) showed that these types
542 of NPF events, or local enhancements of regional NPF events, are common in HTL and that they
543 are linked to roll vortices, which are a specific mode of organized convection in the BL.
544 Figure 9a shows the particle number concentration between 3-10 nm on board the Zeppelin and the
545 airplane as a function of longitude and latitude from HTL on May 8, 2013. The particle number
546 concentration was elevated right over HTL in a narrow sector perpendicular to the mean wind
547 direction. Vertically the sector extended throughout the depth of the ML. The number concentration
548 in the sector increased 2-8 fold compared to the surrounding background number concentration. The
549 mean wind speed in the ML was about 4 m/s and the particle sector was observed throughout the
550 whole measurement flight, for at least 2.5 hours. This suggests that the particle sector was probably
551 at least 35 km long along the mean wind direction.

552 |
553 The concentrated vertical stripes over the growing nucleation mode in Figure 6b were caused by the
554 Zeppelin periodically flying through the particle sector. The sector slowly moved perpendicular to
555 the mean wind towards northeast and when passing over HTL it was seen as the plume of particles
556 in Figure 6d between 07:30-08:00. The particles in the sector grew at approximately the same rate
557 with the background NPF event particles, which also suggests that the particles were formed
558 simultaneously inside the long and narrow sector. Lampilahti et al. (2020b) showed that these types
559 of NPF events, or local enhancements of regional NPF events, are common in HTL and that they
560 are linked to roll vortices, which are a specific mode of organized convection in the BL.

561 |
562 On June 28, 2012 in SPC the Zeppelin flew the measurement profiles over a small area and
563 therefore it was difficult to infer the horizontal extent of the NPF event. However, on June 30, 2012
564 the Zeppelin measured over a larger area in order to find the edges of the airmass where the NPF
565 event was taking place. The flight on June 30, 2012 lasted from 05:00 to 10:00 UTC. Figure 9b
566 shows that the NPF event was observed to occur in the sector of the Valley comprised between
567 Ozzano (just north of the Apennine foothills) and the city of Ferrara (just south of the Po river). The
568 area in between experienced westerly winds, from the inner Po Valley toward the Adriatic sea,
569 which is a common feature of the Po Valley wind breeze system in the early morning.

570 |
571 Farther north of the Po river, an easterly breeze was developing and no NPF was observed (off the
572 map in Figure 8b, see Figure 9). Nocturnal north-easterly breezes are often observed over the Three
573 Venezie Plain as a result of a low-level jet (Camuffo et al., 1979). The variability in local wind
574 fields may generate chemical gradients in the atmospheric surface layer within the Po Valley, hence

575 segregating air masses which can be active or inactive with respect to NPF, in complete absence of
576 orographic forcings (i.e. over a completely flat terrain). Probably the air masses with an easterly
577 component reaching the Zeppelin from the Venetian plain picked up pollution (e.g. CO, NO_x) from
578 urban sources, but we can also speculate that for example ammonia and amines were much lower
579 than in the westerly air masses flowing south of the Po river, which had crossed the areas between
580 Emilia and Lombardy where most agricultural activities take place (see Figure 9). A chemical
581 transport model run predicting NH₃ concentrations with adequate resolution, and using them as a
582 tracer for the actual precursors for NPF, might clarify this point. However modeling atmospheric
583 transport at this scale in an environment like Po Valley can have substantial uncertainties (Vogel and
584 Elbern, 2021).

585 ~~On June 28, 2012 in SPC the Zeppelin flew the measurement profiles over a small area and~~
586 ~~therefore it was difficult to infer the horizontal extent of the NPF event. However, on June 30, 2012~~
587 ~~the Zeppelin measured over a larger area in order to find the edges of the airmass where the NPF~~
588 ~~event was taking place. The flight on June 30, 2012 lasted from 05:00 to 10:00 UTC. Figure 9b~~
589 ~~shows that the NPF event was observed to occur in the sector of the Valley comprised between~~
590 ~~Ozzano (just north of the Apennine foothills) and the city of Ferrara (just south of the Po river). The~~
591 ~~area in between experienced westerly winds, from the inner Po Valley toward the Adriatic sea,~~
592 ~~which is a common feature of the Po Valley wind breeze system in the early morning.~~

593 |

594 ~~**Farther north of the Po river, an easterly breeze was developing and no NPF was observed (off**~~
595 ~~**the map in Figure 9b, see Figure 10). Nocturnal north-easterly breezes are often observed over**~~
596 ~~**the Three Venezie Plain as a result of a low-level jet (Camuffo et al., 1979). The variability in**~~
597 ~~**local wind fields may generate chemical gradients in the atmospheric surface layer within the**~~
598 ~~**Po Valley, hence segregating air masses which can be active or inactive with respect to NPF, in**~~
599 ~~**complete absence of orographic forcings (i.e. over a completely flat terrain). Probably the air**~~
600 ~~**masses with an easterly component reaching the Zeppelin from the Venetian plain picked up**~~
601 ~~**pollution (e.g. CO, NO_x) from urban sources, but we can also speculate that for example**~~
602 ~~**ammonia and amines were much lower than in the westerly air masses flowing south of the Po**~~
603 ~~**river, which had crossed the areas between Emilia and Lombardy where most agricultural**~~
604 ~~**activities take place (see Figure 10). A chemical transport model run predicting NH₃**~~
605 ~~**concentrations with adequate resolution, and using them as a tracer for the actual precursors**~~
606 ~~**for NPF, might clarify this point. However modeling atmospheric transport at this scale in an**~~
607 ~~**environment like Po Valley can have substantial uncertainties (Vogel and Elbern, 2021).**~~

608 |

609 |

610 | **4 Conclusions**

611

612 Flight measurements are essential to evaluate the representativeness of the ground-based in-situ
613 measurements. In many cases it may be impossible to tell from only ground-based data what drives
614 the observed NPF, especially when the effect of BL dynamics is important. Atmospheric models
615 require field observations for validation and constraints. Airborne measurements such as the ones
616 reported here provide valuable data for this purpose.

617

618 We compared case studies from two different environments where NPF occurs frequently: a
619 suburban area in Po Valley, Italy, and a boreal forest in Hyytiälä, Finland. We aimed to answer in
620 which part of the BL the onset of NPF and the growth of the freshly formed particles took place and
621 studied the vertical and horizontal extent of NPF.

622 ~~We compared two different environments where NPF occurs frequently: a suburban area in Po-~~
623 ~~Valley, Italy, and a boreal forest in Hyytiälä, Finland. We aimed to answer in which part of the BL-~~
624 ~~the onset of NPF and the growth of the freshly formed particles takes place and studied the vertical-~~
625 ~~and horizontal extent of NPF.~~

626 |

627 To detect directly the very first steps of NPF in the BL, we used airborne Zeppelin and airplane
628 measurements, supported by ground-based in-situ measurements. The Zeppelin measurements
629 allowed us to study the vertical extent of NPF in the BL. The high time resolution and low cut-off
630 size of the instruments on board allowed us to observe the starting time, location and altitude of an
631 NPF event.

632

633 Within the limits of the Zeppelin's vertical profiling speed (~ 0.5 m/s ascend) and the time
634 resolution of the NAIS, we observed that the onset of NPF happened simultaneously inside the ML.
635 However particles formed close to the surface could probably still be mixed by strong updrafts fast
636 enough so that the number concentrations measured on board the Zeppelin appear homogeneous.
637 The newly formed particles were observed to grow to larger sizes at the same rate within the ML.
638 However, in HTL we observed local enhancements in NPF that were induced by roll vortices in the
639 BL.

640 |

641 In addition a separate layer of sub-10 nm particles was observed above the ML in HTL. Lampilahti
642 et al. (2021) showed that such layers in HTL are likely the result of NPF in the topmost part of the

643 RL. Furthermore it was estimated that around 42% of the NPF events observed in HTL at the
644 surface are entrained from such elevated layers. In SPC we observed how NPF could be happening
645 in one air mass but be completely absent in an adjacent air mass with a different origin.
646 Within the limits of the Zeppelin's vertical profiling speed (~0.5 m/s ascend) and the time-
647 resolution of the NAIS, we observed that the onset of NPF happened simultaneously inside the ML.
648 However particles formed close to the surface could probably still be mixed by strong updrafts fast
649 enough so that the number concentrations measured on board the Zeppelin appear homogeneous.
650 The newly formed particles were observed to grow to larger sizes at the same rate within the ML.
651 However, in HTL we observed local enhancements in NPF that were induced by roll vortices in the
652 BL.

653 |
654 In addition a separate layer of sub-10 nm particles was observed above the ML in HTL. Lampilahti
655 et al. (2020b) showed that such layers in HTL are likely the result of NPF in the topmost part of the
656 RL. Furthermore it was estimated that around 42% of the NPF events observed in HTL at the
657 surface are entrained from such elevated layers. In SPC we observed how NPF could be happening
658 in one air mass but be completely absent in an adjacent air mass with a different origin.

659 |
660 We presented three case studies (two from Italy and one from Finland). The conditions on our case
661 study days represent the typical conditions in these locations when NPF events usually occur. That
662 is to say, a sunny day with the air masses originating from a certain area during a specific
663 timeperiod of the year (May in HTL and June in SPC) when NPF is common. Nevertheless it is not
664 certain that our case studies represent a typical ~~#~~ NPF event days. NPF events also occur under
665 different kinds of conditions. The growing nucleation mode particles originating from NPF do not
666 always grow smoothly and continuously in the measured size distribution like in our cases, but may
667 have large variation and discontinuities, which may reflect the vertical and horizontal variability in
668 NPF.

669 **Acknowledgements**

670 |
671 This research was supported by the European Commission under the Framework Programme 7
672 (FP7-ENV-2010-265148). The support by the Academy of Finland Centre of Excellence program
673 (project no. 272041 and 1118615), the ERC-Advanced "ATMNUCLE" (grant no. 227463), the
674 Eurostars Programme (contract no. E!6911), and the Finnish Cultural Foundation is also gratefully
675 acknowledged. The Zeppelin is accompanied by an international team of scientists and technicians.
676 They are all warmly acknowledged.

677 **Data availability.** Data used in this study is available from different sources: Ground-based
678 meteorological data, radiation, gas and particle size distribution data from HTL (Junninen et al.,
679 2009), the Cessna dataset (Lampilahti et al., 2020a) and the rest of the data (Lampilahti et al.,
680 2021b).

681 ~~This research was supported by the European Commission under the Framework Programme 7~~
682 ~~(FP7-ENV-2010-265148). The support by the Academy of Finland Centre of Excellence program~~
683 ~~(project no. 272041 and 1118615), the ERC-Advanced "ATMNUCLE" (grant no. 227463), the~~
684 ~~Eurostars Programme (contract no. E!6911), and the Finnish Cultural Foundation is also gratefully~~
685 ~~acknowledged. The Zeppelin is accompanied by an international team of scientists and technicians.~~
686 ~~They are all warmly acknowledged.~~

687 |
688 ~~**Data availability.** Ground-based meteorological data, radiation, gas and particle size distribution~~
689 ~~data from HTL is available from <https://smear.avaa.csc.fi/> (last access: Apr 1, 2021). The Cessna~~
690 ~~dataset is available from <https://doi.org/10.5281/zenodo.3688471> (last access: Oct 23, 2020). The~~
691 ~~rest of the data used was gathered into another dataset: <https://doi.org/10.5281/zenodo.4660145>.~~
692 |

693 **Author contributions.** HM, TN, SM, ME, IP, SS, JKa, EJ, TYJ, RK, KLeh, SD, AM, RT, DW, FR,
694 TP, TM and MK coordinated the Zeppelin campaign. RV carried out the Cessna measurements. JLa,
695 TN, HM, JKo, KLei and VMK analyzed and interpreted the data. JL and HM prepared the
696 manuscript, with contributions from all coauthors.

697

698 **The authors declare that they have no conflict of interest.**

699

Aalto, P., Hämeri, K., Becker, E., Weber, R., Salm, J., Mäkelä, J. M., Hoell, C., O'Dowd, C. D., Hansson, H.-C., Väkevää, M., Koponen, I. K., Buzorius, G., and Kulmala, M.: Physical characterization of aerosol particles during nucleation events, *Tellus B*, 53(4), 344–358, <https://doi.org/10.3402/tellusb.v53i4.17127>, 2001.

[Almeida, J., Schobesberger, S., Kürten, A., Ortega, I. K., Kupiainen-Määttä, O., Praplan, A. P., Adamov, A., Amorim, A., Bianchi, F., Breitenlechner, M., David, A., Dommen, J., Donahue, N. M., Downard, A., Dunne, E., Duplissy, J., Ehrhart, S., Flagan, R. C., Franchin, A., Guida, R., Hakala, J., Hansel, A., Heinritzi, M., Henschel, H., Jokinen, T., Junninen, H., Kajos, M., Kangasluoma, J., Keskinen, H., Kupc, A., Kurtén, T., Kvashin, A. N., Laaksonen, A., Lehtipalo, K., Leiminger, M., Leppä, J., Loukonen, V., Makhmutov, V., Mathot, S., McGrath, M. J., Nieminen, T., Olenius, T., Onnela, A., Petäjä, T., Riccobono, F., Riipinen, I., Rissanen, M., Rondo, L., Ruuskanen, T., Santos, F. D., Sarnela, N., Schallhart, S., Schnitzhofer, R., Seinfeld, J. H., Simon, M., Sipilä, M., Stozhkov, Y., Stratmann, F., Tomé, A., Tröstl, J., Tsagkogeorgas, G., Vaattovaara, P., Viisanen, Y., Virtanen, A., Vrtala, A., Wagner, P. E., Weingartner, E., Wex, H., Williamson, C., Wimmer, D., Ye, P., Yli-Juuti, T., Carslaw, K. S., Kulmala, M., Curtius, J., Baltensperger, U., Worsnop, D. R., Vehkamäki, H., and Kirkby, J.: Molecular understanding of sulphuric acid-amine particle nucleation in the atmosphere, *Nature*, 502, 359–363, <https://doi.org/10.1038/nature12663>, 2013.](#)

Camuffo, D., Tampieri, F., and Zambon, G.: Local mesoscale circulation over Venice as a result of the mountain-sea interaction, *Bound.-Layer Meteorol.*, 16(4), 83–92, <https://doi.org/10.1007/BF02220408>, 1979.

Chen, H., Hodshire, A. L., Ortega, J., Greenberg, J., McMurry, P. H., Carlton, A. G., Pierce, J. R., Hanson, D. R., and Smith, J. N.: Vertically resolved concentration and liquid water content of atmospheric nanoparticles at the US DOE Southern Great Plains site, *Atmospheric Chem. Phys.*, 18(4), 311–326, [doi:https://doi.org/10.5194/acp-18-311-2018](https://doi.org/10.5194/acp-18-311-2018), 2018.

[Dada, L., Paasonen, P., Nieminen, T., Buenrostro Mazon, S., Kontkanen, J., Peräkylä, O., Lehtipalo, K., Hussein, T., Petäjä, T., Kerminen, V.-M., Bäck, J., and Kulmala, M.: Long-term analysis of clear-sky new particle formation events and nonevents in Hyytiälä, *Atmos Chem Phys*, 17, 6227–6241, <https://doi.org/10.5194/acp-17-6227-2017>, 2017.](#)

Dal Maso, M., Kulmala, M., Riipinen, I., Wagner, R., Hussein, T., Aalto, P. P., and Lehtinen, K. E.: Formation and growth of fresh atmospheric aerosols: eight years of aerosol size distribution data from SMEAR II, Hyytiälä, Finland, *Boreal Environ. Res.*, 10(5), 323, 2005.

[Dunne, E. M., Gordon, H., Kürten, A., Almeida, J., Duplissy, J., Williamson, C., Ortega, I. K., Pringle, K. J., Adamov, A., Baltensperger, U., Barmet, P., Benduhn, F., Bianchi, F., Breitenlechner, M., Clarke, A., Curtius, J., Dommen, J., Donahue, N. M., Ehrhart, S., Flagan, R. C., Franchin, A., Guida, R., Hakala, J., Hansel, A., Heinritzi, M., Jokinen, T., Kangasluoma, J., Kirkby, J., Kulmala, M., Kupc, A., Lawler, M. J., Lehtipalo, K., Makhmutov, V., Mann, G., Mathot, S., Merikanto, J., Miettinen, P., Nenes, A., Onnela, A., Rap, A., Reddington, C. L. S., Riccobono, F., Richards, N. A. D., Rissanen, M. P., Rondo, L., Sarnela, N., Schobesberger, S., Sengupta, K., Simon, M., Sipilä, M., Smith, J. N., Stozhkov, Y., Tomé, A., Tröstl, J., Wagner, P. E., Wimmer, D., Winkler, P. M., Worsnop, D. R., and Carslaw, K. S.: Global atmospheric particle formation from CERN CLOUD measurements, *Science*, 354, 1119–1124, <https://doi.org/10.1126/science.aaf2649>, 2016.](#)

- Ehn, M., Junninen, H., Petäjä, T., Kurtén, T., Kerminen, V.-M., Schobesberger, S., Manninen, H. E., Ortega, I. K., Vehkamäki, H., Kulmala, M., and Worsnop, D. R.: Composition and temporal behavior of ambient ions in the boreal forest, *Atmospheric Chem. Phys.*, 10(17), 8513–8530, [doi:https://doi.org/10.5194/acp-10-8513-2010](https://doi.org/10.5194/acp-10-8513-2010), 2010.
- Ehn, M., Thornton, J. A., Kleist, E., Sipilä, M., Junninen, H., Pullinen, I., Springer, M., Rubach, F., Tillmann, R., Lee, B., Lopez-Hilfiker, F., Andres, S., Acir, I.-H., Rissanen, M., Jokinen, T., Schobesberger, S., Kangasluoma, J., Kontkanen, J., Nieminen, T., Kurtén, T., Nielsen, L. B., Jørgensen, S., Kjaergaard, H. G., Canagaratna, M., Maso, M. D., Berndt, T., Petäjä, T., Wahner, A., Kerminen, V.-M., Kulmala, M., Worsnop, D. R., Wildt, J., and Mentel, T. F.: A large source of low-volatility secondary organic aerosol, *Nature*, 506(7489), 476–479, <https://doi.org/10.1038/nature13032>, 2014.
- Eisele, F. L. and Tanner, D. J.: Ion-assisted tropospheric OH measurements, *J. Geophys. Res. Atmospheres*, 96(D5), 9295–9308, <https://doi.org/10.1029/91JD00198>, 1991.
- [Gordon, H., Kirkby, J., Baltensperger, U., Bianchi, F., Breitenlechner, M., Curtius, J., Dias, A., Dommen, J., Donahue, N. M., Dunne, E. M., Duplissy, J., Ehrhart, S., Flagan, R. C., Frege, C., Fuchs, C., Hansel, A., Hoyle, C. R., Kulmala, M., Kürten, A., Lehtipalo, K., Makhmutov, V., Molteni, U., Rissanen, M. P., Stozkhov, Y., Tröstl, J., Tsagkogeorgas, G., Wagner, R., Williamson, C., Wimmer, D., Winkler, P. M., Yan, C., and Carslaw, K. S.: Causes and importance of new particle formation in the present-day and preindustrial atmospheres, *J. Geophys. Res. Atmospheres*, 122, 8739–8760, <https://doi.org/10.1002/2017JD026844>, 2017.](https://doi.org/10.1002/2017JD026844)
- Hakola, H., Tarvainen, V., Laurila, T., Hiltunen, V., Hellén, H., and Keronen, P.: Seasonal variation of VOC concentrations above a boreal coniferous forest, *Atmos. Environ.*, 37(12), 1623–1634, [https://doi.org/10.1016/S1352-2310\(03\)00014-1](https://doi.org/10.1016/S1352-2310(03)00014-1), 2003.
- Hamed, A., Joutsensaari, J., Mikkonen, S., Sogacheva, L., Maso, M. D., Kulmala, M., Cavalli, F., Fuzzi, S., Facchini, M. C., Decesari, S., Mircea, M., Lehtinen, K. E. J., and Laaksonen, A.: Nucleation and growth of new particles in Po Valley, Italy, *Atmospheric Chem. Phys.*, 7(2), 355–376, [doi:https://doi.org/10.5194/acp-7-355-2007](https://doi.org/10.5194/acp-7-355-2007), 2007.
- Hari, P. and Kulmala, M.: Station for measuring ecosystem-atmosphere relations (SMEAR II), *Boreal Environ. Res.*, 10(5), 315–322, 2005.
- [Jäger, J.: Airborne VOC measurements on board the Zeppelin NT during the PEGASOS campaigns in 2012 deploying the improved Fast-GC-MSD System, Forschungszentrum Jülich GmbH, 2014.](https://www.fz-juelich.de/ia/ia-1/~/media/ia-1/PDF/airborne_voc_measurements_on_board_the_zeppelin_nt_during_the_pegasos_campaigns_in_2012_deploying_the_improved_fast-gc-msd_system.pdf)
- [Junkermann, W. and Hacker, J. M.: Ultrafine Particles in the Lower Troposphere: Major Sources, Invisible Plumes, and Meteorological Transport Processes, *Bull. Am. Meteorol. Soc.*, 99, 2587–2602, <https://doi.org/10.1175/BAMS-D-18-0075.1>, 2018.](https://doi.org/10.1175/BAMS-D-18-0075.1)
- [Junninen, H., Lauri, A., Keronen, P., Aalto, P., Hiltunen, V., Hari, P., and Kulmala, M.: Smart-SMEAR: on-line data exploration and visualization tool for SMEAR stations., *Boreal Environ. Res.*, 14, 447–457, 2009.](https://doi.org/10.1175/BAMS-D-18-0075.1)
- Junninen, H., Ehn, M., Petäjä, T., Luosujärvi, L., Kotiaho, T., Kostianen, R., Rohner, U., Gonin, M., Fuhrer, K., Kulmala, M., and Worsnop, D. R.: A high-resolution mass spectrometer to measure atmospheric ion composition, *Atmospheric Meas. Tech.*, 3(4), 1039–1053, <https://doi.org/10.5194/amt-3-1039-2010>, 2010.

- Kerminen, V.-M., Chen, X., Vakkari, V., Petäjä, T., Kulmala, M., and Bianchi, F.: Atmospheric new particle formation and growth: review of field observations, *Environ. Res. Lett.*, 13(10), 103003, <https://doi.org/10.1088/1748-9326/aadf3c>, 2018.
- [Kirkby, J., Curtius, J., Almeida, J., Dunne, E., Duplissy, J., Ehrhart, S., Franchin, A., Gagné, S., Ickes, L., Kürten, A., Kupc, A., Metzger, A., Riccobono, F., Rondo, L., Schobesberger, S., Tsagkogeorgas, G., Wimmer, D., Amorim, A., Bianchi, F., Breitenlechner, M., David, A., Dommen, J., Downard, A., Ehn, M., Flagan, R. C., Haider, S., Hansel, A., Hauser, D., Jud, W., Junninen, H., Kreissl, F., Kvashin, A., Laaksonen, A., Lehtipalo, K., Lima, J., Lovejoy, E. R., Makhmutov, V., Mathot, S., Mikkilä, J., Minginette, P., Mogo, S., Nieminen, T., Onnela, A., Pereira, P., Petäjä, T., Schnitzhofer, R., Seinfeld, J. H., Sipilä, M., Stozhkov, Y., Stratmann, F., Tomé, A., Vanhanen, J., Viisanen, Y., Vrtala, A., Wagner, P. E., Walther, H., Weingartner, E., Wex, H., Winkler, P. M., Carslaw, K. S., Worsnop, D. R., Baltensperger, U., and Kulmala, M.: Role of sulphuric acid, ammonia and galactic cosmic rays in atmospheric aerosol nucleation, *Nature*, 476, 429–433, <https://doi.org/10.1038/nature10343>, 2011.](#)
- Kontkanen, J., Järvinen, E., Manninen, H. E., Lehtipalo, K., Kangasluoma, J., Decesari, S., Gobbi, G. P., Laaksonen, A., Petäjä, T., and Kulmala, M.: High concentrations of sub-3nm clusters and frequent new particle formation observed in the Po Valley, Italy, during the PEGASOS 2012 campaign, [doi:http://dx.doi.org/10.5194/acp-16-1919-2016](http://dx.doi.org/10.5194/acp-16-1919-2016), 2016.
- Kulmala, M., Petäjä, T., Nieminen, T., Sipilä, M., Manninen, H. E., Lehtipalo, K., Dal Maso, M., Aalto, P. P., Junninen, H., Paasonen, P., Riipinen, I., Lehtinen, K. E. J., Laaksonen, A., and Kerminen, V.-M.: Measurement of the nucleation of atmospheric aerosol particles, *Nat. Protoc.*, 7(9), 1651–1667, <https://doi.org/10.1038/nprot.2012.091>, 2012.
- Kulmala, M., Kontkanen, J., Junninen, H., Lehtipalo, K., Manninen, H. E., Nieminen, T., Petäjä, T., Sipilä, M., Schobesberger, S., Rantala, P., Franchin, A., Jokinen, T., Järvinen, E., Äijälä, M., Kangasluoma, J., Hakala, J., Aalto, P. P., Paasonen, P., Mikkilä, J., Vanhanen, J., Aalto, J., Hakola, H., Makkonen, U., Ruuskanen, T., Mauldin, R. L., Duplissy, J., Vehkamäki, H., Back, J., Kortelainen, A., Riipinen, I., Kurten, T., Johnston, M. V., Smith, J. N., Ehn, M., Mentel, T. F., Lehtinen, K. E. J., Laaksonen, A., Kerminen, V.-M., and Worsnop, D. R.: Direct observations of atmospheric aerosol nucleation, *Science*, 339(6122), 943–946, <https://doi.org/10.1126/science.1227385>, 2013.
- Laakso, L., Grönholm, T., Kulmala, L., Haapanala, S., Hirsikko, A., Lovejoy, E. R., Kazil, J., Kurten, T., Boy, M., Nilsson, E. D., Sogachev, A., Riipinen, I., Stratmann, F., and Kulmala, M.: Hot-air balloon as a platform for boundary layer profile measurements during particle formation, *Boreal Environ. Res.*, 12(3), 279–294, 2007.
- Laaksonen, A., Hamed, A., Joutsensaari, J., Hiltunen, L., Cavalli, F., Junkermann, W., Asmi, A., Fuzzi, S., and Facchini, M. C.: Cloud condensation nucleus production from nucleation events at a highly polluted region, *Geophys. Res. Lett.*, 32, <https://doi.org/10.1029/2004GL022092>, 2005.
- [Lampilahti, J., Manninen, H. E., Leino, K., Väänänen, R., Manninen, A., Buenrostro Mazon, S., Nieminen, T., Leskinen, M., Enroth, J., Bister, M., Zilitinkevich, S., Kangasluoma, J., Järvinen, H., Kerminen, V.-M., Petäjä, T., and Kulmala, M.: Data set of airborne and ground-based atmospheric measurements from Hyytiälä, Finland, <https://doi.org/10.5281/zenodo.3688471>, 2020a.](#)
- [Lampilahti, J., Manninen, H. E., Leino, K., Väänänen, R., Manninen, A., Buenrostro Mazon, S., Nieminen, T., Leskinen, M., Enroth, J., Bister, M., Zilitinkevich, S., Kangasluoma, J., Järvinen, H.,](#)

- [Kerminen, V.-M., Petäjä, T., and Kulmala, M.: Roll vortices induce new particle formation bursts in the planetary boundary layer, *Atmospheric Chem. Phys.*, **20**, 11841–11854, <https://doi.org/10.5194/acp-20-11841-2020>, 2020b.](https://doi.org/10.5194/acp-20-11841-2020)
- Lampilahti, J., Leino, K., Manninen, A., Poutanen, P., Franck, A., Peltola, M., Hietala, P., Beck, L., Dada, L., Quéléver, L., Öhrnberg, R., Zhou, Y., Ekblom, M., Vakkari, V., Zilitinkevich, S., Kerminen, V.-M., Petäjä, T., and Kulmala, M.: Aerosol particle formation in the upper residual layer, *Atmospheric Chem. Phys.*, **21**, 7901–7915, ~~Discuss.~~, ~~1–24~~, [doi:https://doi.org/10.5194/acp-21-7901-2021](https://doi.org/10.5194/acp-21-7901-2021)020-923, 20210a.
- [Lampilahti, J., Manninen, H. E., Nieminen, T., Mirme, S., Ehn, M., Pullinen, I., Leino, K., Schobesberger, S., Kangasluoma, J., Kontkanen, J., Järvinen, E., Väänänen, R., Yli-Juuti, T., Krecji, R., Lehtipalo, K., Levula, J., Mirme, A., Decesari, S., Tillmann, R., Worsnop, D. R., Rohrer, F., Petäjä, T., Kerminen, V.-M., Mentel, T. F., and Kulmala, M.: Zeppelin-led study on the onset of new particle formation in the planetary boundary layer: dataset, <https://doi.org/10.5281/zenodo.4660145>, 2021b.](https://doi.org/10.5281/zenodo.4660145)
- ~~Lampilahti, J., Manninen, H. E., Leino, K., Väänänen, R., Manninen, A., Buenrostro Mazon, S., Nieminen, T., Leskinen, M., Enroth, J., Bister, M., Zilitinkevich, S., Kangasluoma, J., Järvinen, H., Kerminen, V.-M., Petäjä, T. and Kulmala, M.: Roll vortices induce new particle formation bursts in the planetary boundary layer, *Atmospheric Chem. Phys.*, **20**(20), 11841–11854, [doi:https://doi.org/10.5194/acp-20-11841-2020](https://doi.org/10.5194/acp-20-11841-2020), 2020b.~~
- Lehtipalo, K., Leppä, J., Kontkanen, J., Kangasluoma, J., Franchin, A., Wimmer, D., Schobesberger, S., Junninen, H., Petäjä, T., Sipilä, M., Mikkilä, J., Vanhanen, J., Worsnop, D. R., and Kulmala, M.: Methods for determining particle size distribution and growth rates between 1 and 3 nm using the Particle Size Magnifier, *Boreal Environ. Res.*, **19**, 22, 2014.
- Leino, K., Nieminen, T., Manninen, H. E., Petäjä, T., Kerminen, V.-M., and Kulmala, M.: Intermediate ions as a strong indicator for new particle formation bursts in boreal forest, *Boreal Environ. Res.*, **21**, 274–286, 2016.
- Leino, K., Lampilahti, J., Poutanen, P., Väänänen, R., Manninen, A., Buenrostro Mazon, S., Dada, L., Franck, A., Wimmer, D., Aalto, P. P., Ahonen, L. R., Enroth, J., Kangasluoma, J., Keronen, P., Korhonen, F., Laakso, H., Matilainen, T., Siivola, E., Manninen, H. E., Lehtipalo, K., Kerminen, V.-M., Petäjä, T., and Kulmala, M.: Vertical profiles of sub-3 nm particles over the boreal forest, *Atmospheric Chem. Phys.*, **19**(6), 4127–4138, <https://doi.org/10.5194/acp-19-4127-2019>, 2019.
- Manninen, H. E., Petäjä, T., Asmi, E., Riipinen, N., Nieminen, T., Mikkilä, J., Horrak, U., Mirme, A., Mirme, S., Laakso, L., Kerminen, V.-M., and Kulmala, M.: Long-term field measurements of charged and neutral clusters using Neutral cluster and Air Ion Spectrometer (NAIS), *Boreal Environ. Res.*, **14**(4), 591–605, 2009.
- Mirme, S. and Mirme, A.: The mathematical principles and design of the NAIS – a spectrometer for the measurement of cluster ion and nanometer aerosol size distributions, *Atmospheric Meas. Tech.*, **6**(4), 1061–1071, <https://doi.org/10.5194/amt-6-1061-2013>, 2013.
- [Mohr, C., Thornton, J. A., Heitto, A., Lopez-Hilfiker, F. D., Lutz, A., Riipinen, I., Hong, J., Donahue, N. M., Hallquist, M., Petäjä, T., Kulmala, M., and Yli-Juuti, T.: Molecular identification of organic vapors driving atmospheric nanoparticle growth, *Nat. Commun.*, **10**, 4442, <https://doi.org/10.1038/s41467-019-12473-2>, 2019.](https://doi.org/10.1038/s41467-019-12473-2)

Nieminen, T., Asmi, A., Dal Maso, M., Aalto, P. P., Keronen, P., Petäjä, T., Kulmala, M., and Kerminen, V.-M.: Trends in atmospheric new-particle formation: 16 years of observations in a boreal-forest environment, *Boreal Environ. Res.*, 19, 191–214, 2014.

Nieminen, T., Yli-Juuti, T., Manninen, H. E., Petäjä, T., Kerminen, V.-M., and Kulmala, M.: Technical note: New particle formation event forecasts during PEGASOS–Zeppelin Northern mission 2013 in Hyytiälä, Finland, *Atmospheric Chem. Phys.*, 15(24), 12385–12396, <https://doi.org/10.5194/acp-15-12385-2015>, 2015.

[Nilsson, E. D., Rannik, Ü., Kulmala, M., Buzorius, G., and O’ Dowd, C. D.: Effects of continental boundary layer evolution, convection, turbulence and entrainment, on aerosol formation, *Tellus B*, 53, 441–461, https://doi.org/10.1034/j.1600-0889.2001.530409.x, 2001.](https://doi.org/10.1034/j.1600-0889.2001.530409.x)

[Nilsson, E. D., Paatero, J. and Boy, M.: Effects of air masses and synoptic weather on aerosol formation in the continental boundary layer, *Tellus B*, 53\(4\), 462–478, doi:10.1034/j.1600-0889.2001.530410.x, 2001a.](https://doi.org/10.1034/j.1600-0889.2001.530410.x)

[Nilsson, E. D., Rannik, Ü., Kulmala, M., Buzorius, G. and O’ Dowd, C. D.: Effects of continental boundary layer evolution, convection, turbulence and entrainment, on aerosol formation, *Tellus B*, 53\(4\), 441–461, doi:10.1034/j.1600-0889.2001.530409.x, 2001b.](https://doi.org/10.1034/j.1600-0889.2001.530409.x)

O’Dowd, C. D., Yoon, Y. J., Junkermann, W., Aalto, P., Kulmala, M., Lihavainen, H., and Viisanen, Y.: Airborne measurements of nucleation mode particles II: boreal forest nucleation events, *Atmospheric Chem. Phys.*, 9(3), 937–944, <https://doi.org/10.5194/acp-9-937-2009>, 2009.

[Pierce, J. R. and Adams, P. J.: Uncertainty in global CCN concentrations from uncertain aerosol nucleation and primary emission rates, *Atmospheric Chem. Phys.*, 9, 1339–1356, https://doi.org/10.5194/acp-9-1339-2009, 2009.](https://doi.org/10.5194/acp-9-1339-2009)

Platis, A., Altstädter, B., Wehner, B., Wildmann, N., Lampert, A., Hermann, M., Birmili, W., and Bange, J.: An Observational Case Study on the Influence of Atmospheric Boundary-Layer Dynamics on New Particle Formation, *Bound.-Layer Meteorol.*, 158(1), 67–92, <https://doi.org/10.1007/s10546-015-0084-y>, 2015.

Schobesberger, S., Väänänen, R., Leino, K., Virkkula, A., Backman, J., Pohja, T., Siivola, E., Franchin, A., Mikkilä, J., Paramonov, M., Aalto, P. P., Krejci, R., Petäjä, T., and Kulmala, M.: Airborne measurements over the boreal forest of southern Finland during new particle formation events in 2009 and 2010, *Boreal Environ. Res.*, 18(2), 145–164, 2013.

Siebert, H., Stratmann, F., and Wehner, B.: First observations of increased ultrafine particle number concentrations near the inversion of a continental planetary boundary layer and its relation to ground-based measurements, *Geophys. Res. Lett.*, 31, L09102, <https://doi.org/10.1029/2003GL019086>, 2004.

Sipilä, M., Berndt, T., Petäjä, T., Brus, D., Vanhanen, J., Stratmann, F., Patokoski, J., Mauldin, R. L., Hyvärinen, A.-P., Lihavainen, H., and Kulmala, M.: The Role of Sulfuric Acid in Atmospheric Nucleation, *Science*, 327(5970), 1243–1246, <https://doi.org/10.1126/science.1180315>, 2010.

Sogacheva, L., Hamed, A., Facchini, M. C., Kulmala, M., and Laaksonen, A.: Relation of air mass history to nucleation events in Po Valley, Italy, using back trajectories analysis, *Atmos Chem Phys*, 7(3), 839–853, <https://doi.org/10.5194/acp-7-839-2007>, 2007.

- Sogacheva, L., Saukkonen, L., Nilsson, E. D., Dal Maso, M., Schultz, D. M., De Leeuw, G., and Kulmala, M.: New aerosol particle formation in different synoptic situations at Hyytiälä, Southern Finland, *Tellus B*, 60(4), 485–494, <https://doi.org/10.1111/j.1600-0889.2008.00364.x>, 2008.
- Stein, A. F., Draxler, R. R., Rolph, G. D., Stunder, B. J. B., Cohen, M. D., and Ngan, F.: NOAA's HYSPLIT Atmospheric Transport and Dispersion Modeling System, *Bull. Am. Meteorol. Soc.*, 96(12), 2059–2077, <https://doi.org/10.1175/BAMS-D-14-00110.1>, 2015.
- [Stratmann, F., Siebert, H., Spindler, G., Wehner, B., Althausen, D., Heintzenberg, J., Hellmuth, O., Rinke, R., Schmieder, U., Seidel, C., Tuch, T., Uhrner, U., Wiedensohler, A., Wandinger, U., Wendisch, M., Schell, D., and Stohl, A.: New-particle formation events in a continental boundary layer: first results from the SATURN experiment, *Atmospheric Chem. Phys.*, 3, 1445–1459, <https://doi.org/10.5194/acp-3-1445-2003>, 2003.](https://doi.org/10.5194/acp-3-1445-2003)
- Stull, R. B.: *An Introduction to Boundary Layer Meteorology*, Softcover reprint of the original 1st ed. 1988 edition., Springer, Dordrecht, 670 pp., 1988.
- [Sullivan, A. P., Hodas, N., Turpin, B. J., Skog, K., Keutsch, F. N., Gilardoni, S., Paglione, M., Rinaldi, M., Decesari, S., Facchini, M. C., Poulain, L., Herrmann, H., Wiedensohler, A., Nemitz, E., Twigg, M. M., and Collett Jr., J. L.: Evidence for ambient dark aqueous SOA formation in the Po Valley, Italy, *Atmospheric Chem. Phys.*, 16, 8095–8108, <https://doi.org/10.5194/acp-16-8095-2016>, 2016.](https://doi.org/10.5194/acp-16-8095-2016)
- Väänänen, R., Krejci, R., Manninen, H. E., Manninen, A., Lampilahti, J., Buenrostro Mazon, S., Nieminen, T., Yli-Juuti, T., Kontkanen, J., Asmi, A., Aalto, P. P., Keronen, P., Pohja, T., O'Connor, E., Kerminen, V.-M., Petäjä, T., and Kulmala, M.: Vertical and horizontal variation of aerosol number size distribution in the boreal environment, *Atmospheric Chem. Phys. Discuss.*, Manuscript in review, <https://doi.org/10.5194/acp-2016-556>, 2016.
- Vanhanen, J., Mikkilä, J., Lehtipalo, K., Sipilä, M., Manninen, H. E., Siivola, E., Petäjä, T., and Kulmala, M.: Particle size magnifier for nano-CN detection, *Aerosol Sci. Technol.*, 45(4), 533–542, <https://doi.org/10.1080/02786826.2010.547889>, 2011.
- [Vogel, A. and Elbern, H.: Identifying forecast uncertainties for biogenic gases in the Po Valley related to model configuration in EURAD-IM during PEGASOS 2012, *Atmospheric Chem. Phys.*, 21, 4039–4057, <https://doi.org/10.5194/acp-21-4039-2021>, 2021.](https://doi.org/10.5194/acp-21-4039-2021)
- Wehner, B., Siebert, H., Ansmann, A., Ditas, F., Seifert, P., Stratmann, F., Wiedensohler, A., Apituley, A., Shaw, R. A., Manninen, H. E., and Kulmala, M.: Observations of turbulence-induced new particle formation in the residual layer, *Atmospheric Chem. Phys.*, 10(9), 4319–4330, <https://doi.org/10.5194/acp-10-4319-2010>, 2010.
- Wiedensohler, A., Birmili, W., Nowak, A., Sonntag, A., Weinhold, K., Merkel, M., Wehner, B., Tuch, T., Pfeifer, S., Fiebig, M., Fjåraa, A. M., Asmi, E., Sellegri, K., Depuy, R., Venzac, H., Villani, P., Laj, P., Aalto, P., Ogren, J. A., Swietlicki, E., Williams, P., Roldin, P., Quincey, P., Hüglin, C., Fierz-Schmidhauser, R., Gysel, M., Weingartner, E., Riccobono, F., Santos, S., Gruning, C., Faloon, K., Beddows, D., Harrison, R., Monahan, C., Jennings, S. G., O'Dowd, C. D., Marinoni, A., Horn, H.-G., Keck, L., Jiang, J., Scheckman, J., McMurry, P. H., Deng, Z., Zhao, C. S., Moerman, M., Henzing, B., de Leeuw, G., Löschau, G., and Bastian, S.: Mobility particle size spectrometers: harmonization of technical standards and data structure to facilitate high quality long-term

observations of atmospheric particle number size distributions, Atmospheric Meas. Tech., 5(3), 657–685, <https://doi.org/10.5194/amt-5-657-2012>, 2012.

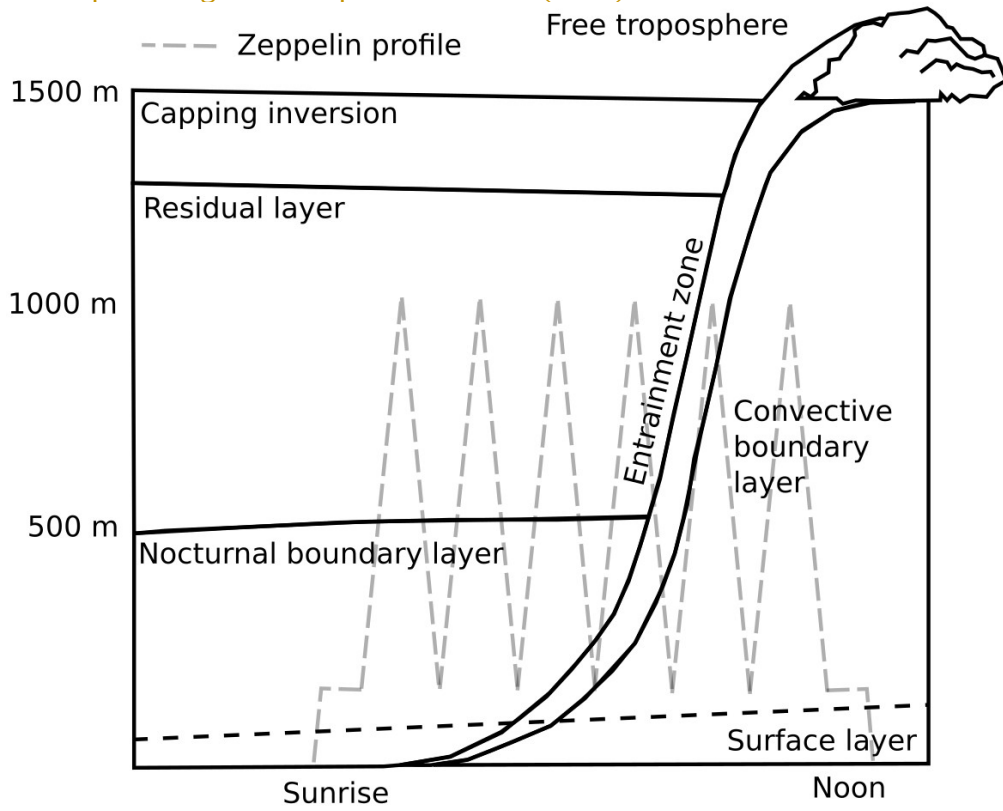
[Yu, F. and Luo, G.: Simulation of particle size distribution with a global aerosol model: contribution of nucleation to aerosol and CCN number concentrations, Atmospheric Chem. Phys., 9, 7691–7710, 2009.](#)

702 |

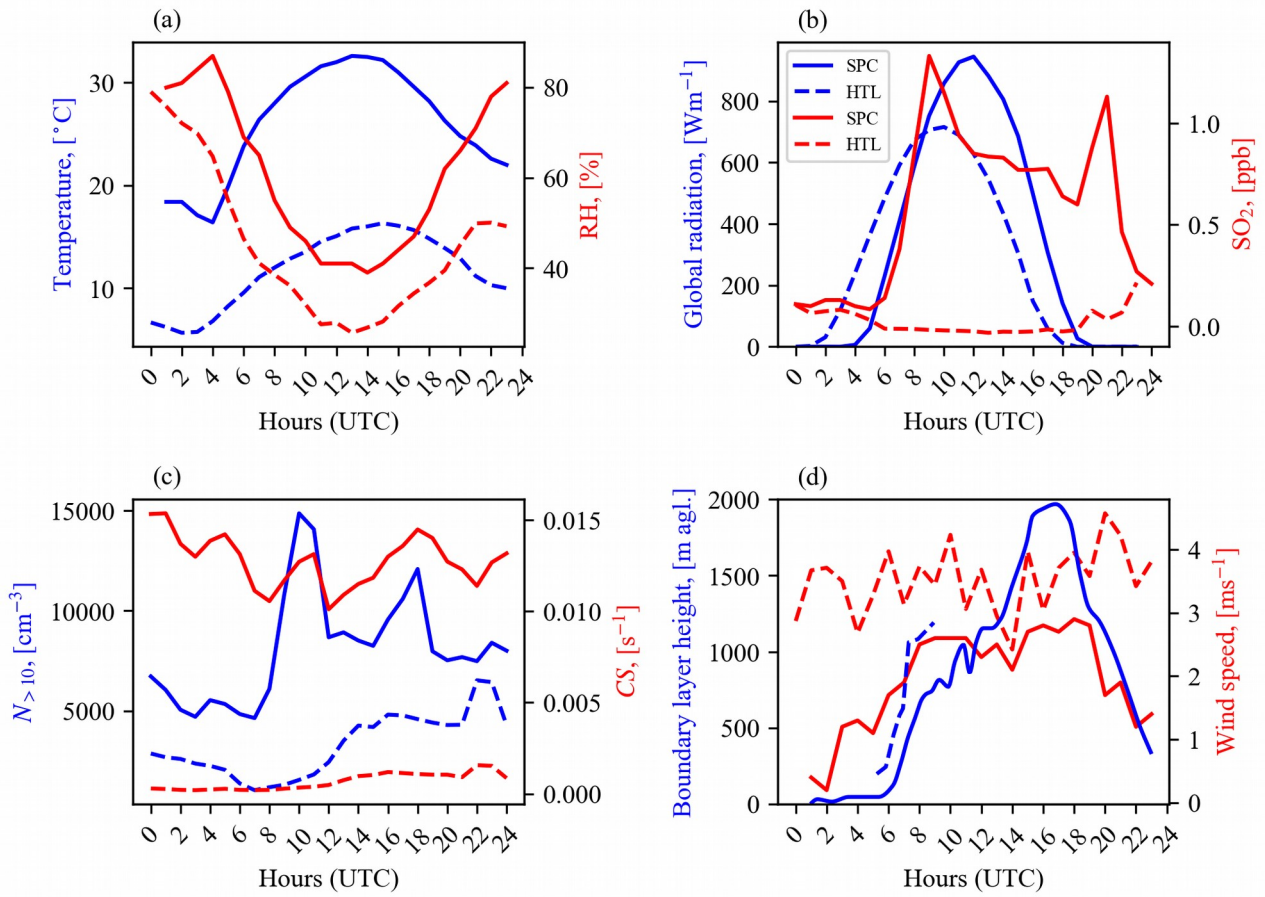
703

704 |

705 | **Figure 1: A schematic diagram of different atmospheric layers in the lower troposphere and their**
706 | **development during the morning hours. A generic Zeppelin measurement profile (dashed gray line)**
707 | **is displayed on top. The figure is adapted from Stull (1988):**

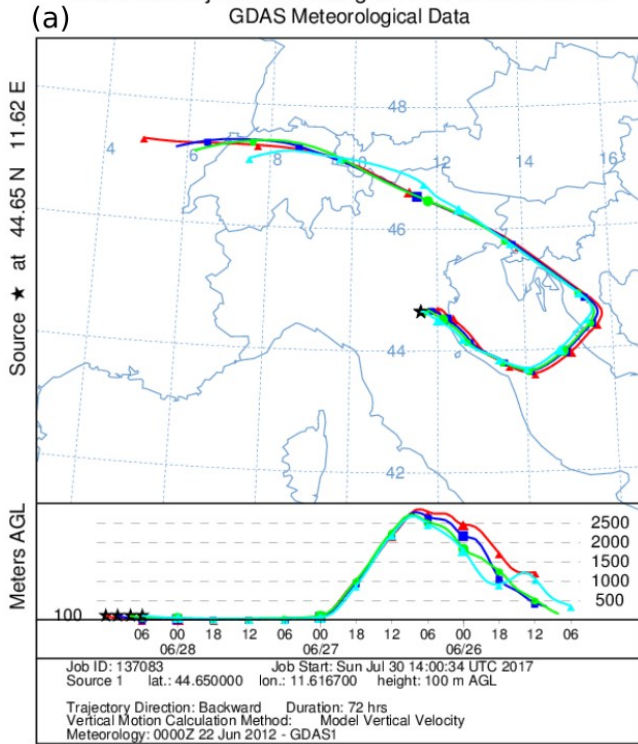


709 | ~~Figure 2: Airmass backward trajectories to (a) SPC during the morning of June 28, 2012 and (b)~~
710 | ~~HFL during the morning of May 8, 2013.~~

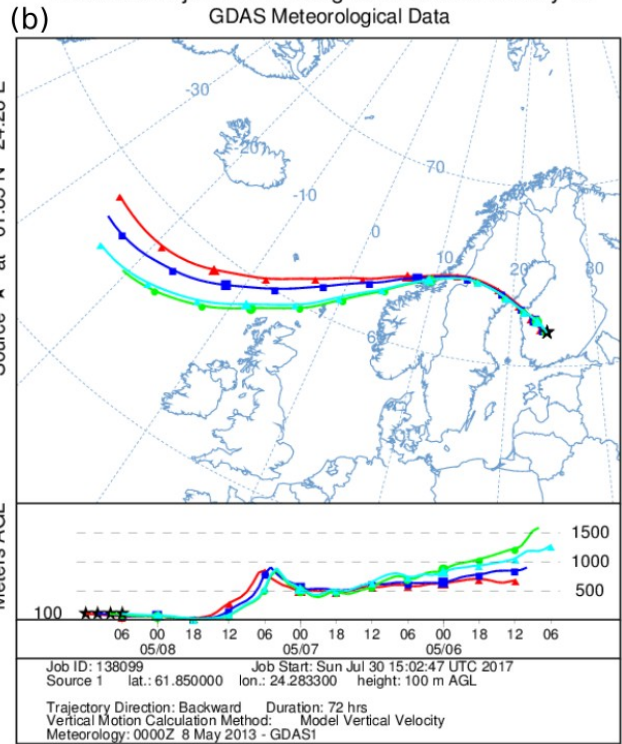


711 Figure 3: Diurnal variation in (a) temperature, relative humidity, (b) global radiation, SO_2 -
 712 concentration, (c) >10 nm particle number concentration, condensation sink (CS) and (d) mixed-
 713 layer height in SPC on June 28, 2012 and in HTL on May 8, 2013.

NOAA HYSPLIT MODEL
 Backward trajectories ending at 1200 UTC 28 Jun 12
 GDAS Meteorological Data



NOAA HYSPLIT MODEL
 Backward trajectories ending at 1200 UTC 08 May 13
 GDAS Meteorological Data



715
 716

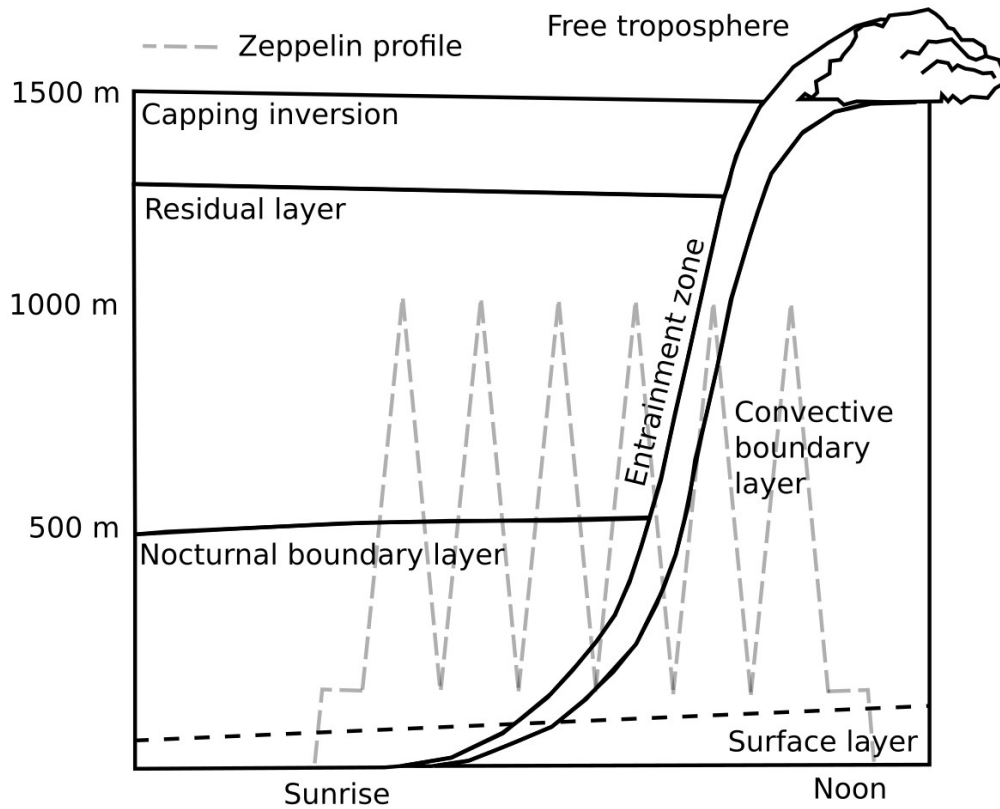


Figure 1: A schematic diagram of different atmospheric layers in the lower troposphere and their development during the morning hours. A generic Zeppelin measurement profile (dashed gray line) is displayed on top. The figure is adapted from Stull (1988)

718 |
719 |

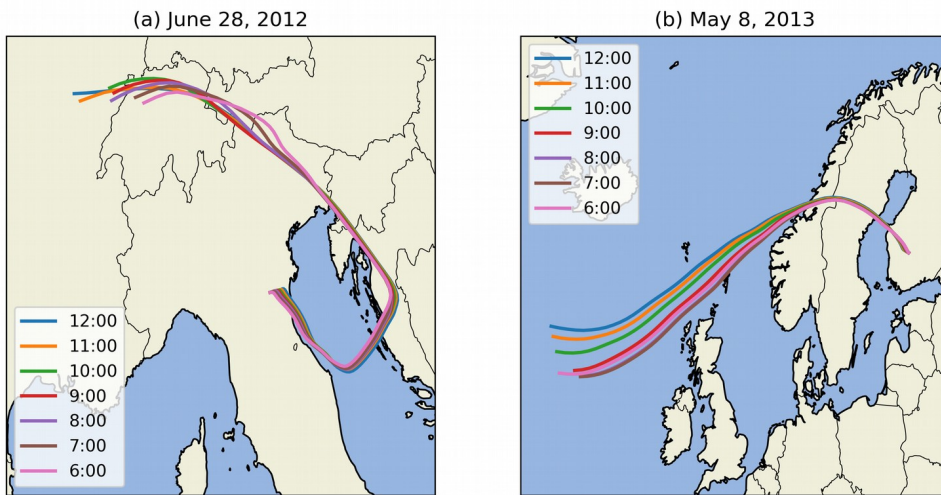


Figure 2: Airmass backward trajectories to (a) SPC during the morning of June 28, 2012 and (b) HTL during the morning of May 8, 2013. The legend shows the hour of airmass arrival in UTC. The arrival altitude was set to 100 m above ground.

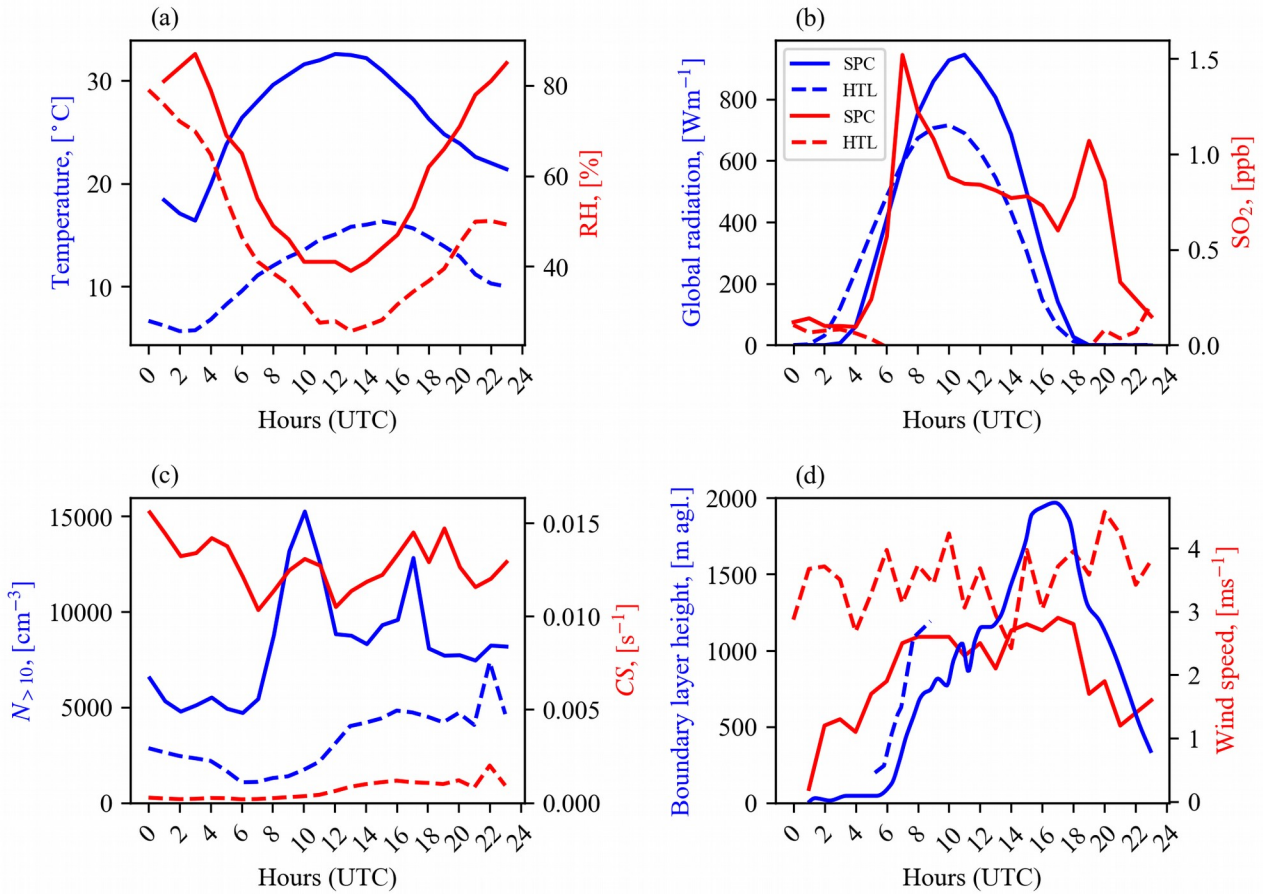


Figure 3: Ground-based measurements of diurnal variation in (a) temperature, relative humidity, (b) global radiation, SO₂ concentration, (c) >10 nm particle number concentration, condensation sink (CS) and (d) mixed layer height in SPC on June 28, 2012 and in HTL on May 8, 2013.

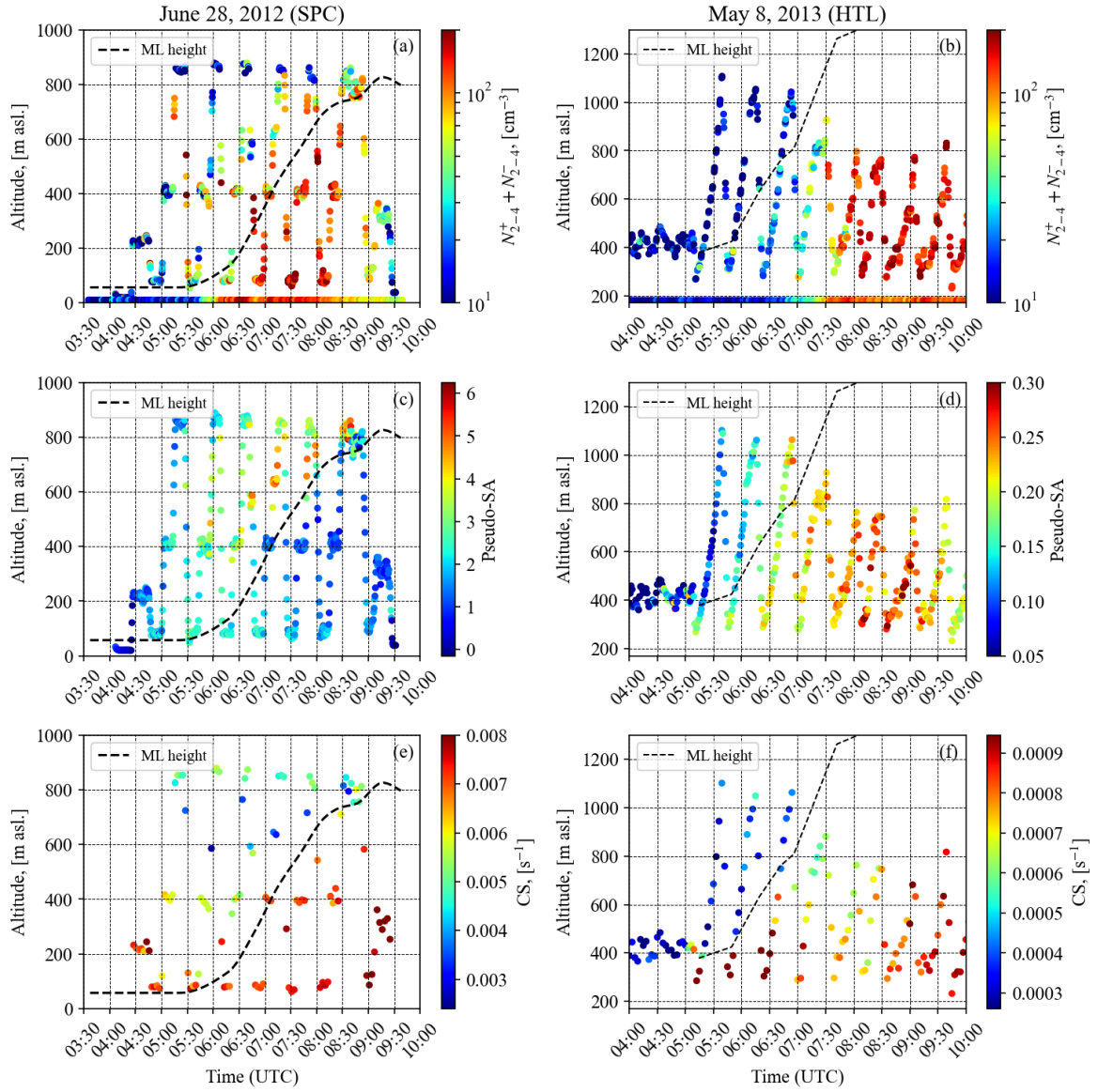


Figure 4: Time-evolution of selected variables as a function of height in SPC on June 28, 2012 and HTL on May 8, 2013. Panels (a) and (b) show the intermediate ion number concentration from SPC and HTL. Ground-based measurements as well as measurements from the Zeppelin are shown. Panels (c) and (d) show the pseudo-SA from SPC and HTL. Panels (e) and (f) show the CS. Height of the mixed layer is shown in all panels.

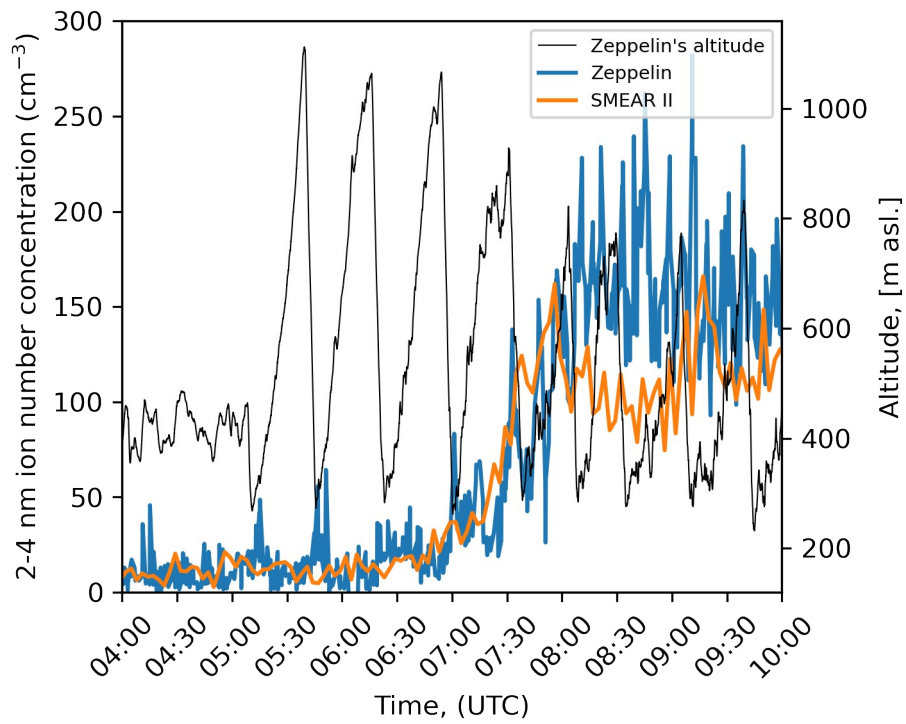


Figure 5: Time series of intermediate (2-4 nm) ion number concentration on board the Zeppelin and the SMEAR II station and the Zeppelin's altitude in HTL on May 8, 2013.

724 | Figure 4: Time-evolution of selected variables as a function of height in SPC and HTL. Panels (a)-
725 | and (b) show the intermediate ion number concentration from SPC and HTL. Ground-based
726 | measurements as well as measurements from the Zeppelin are shown. Panels (c) and (d) show the
727 | pseudo-SA from SPC and HTL. Panels (e) and (f) show the CS. Height of the mixed layer is shown
728 | in all panels.

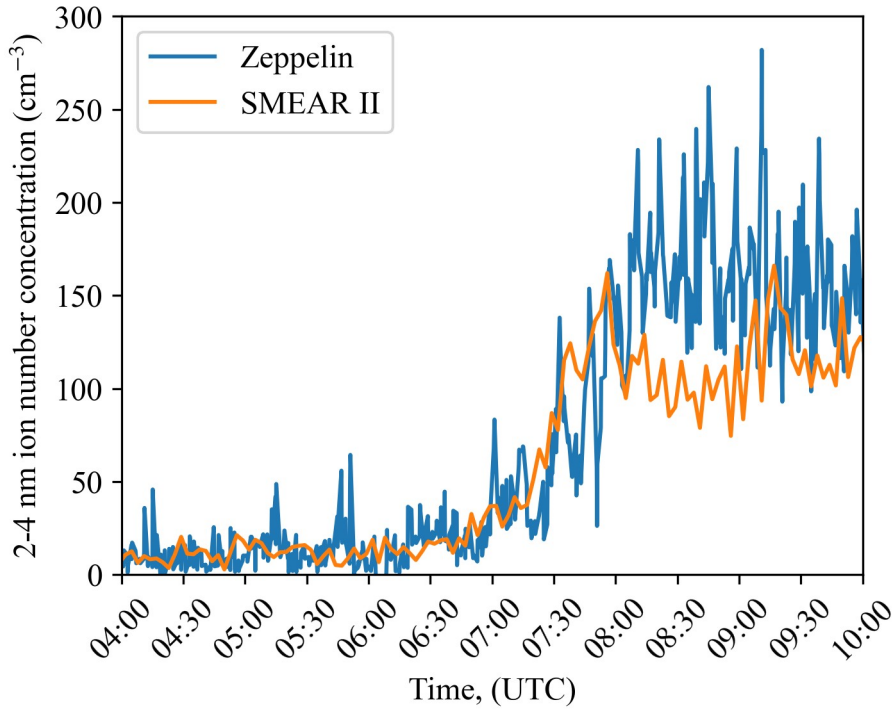


Figure 5: Time series of intermediate (2-4 nm) ion number concentration on board the Zeppelin and

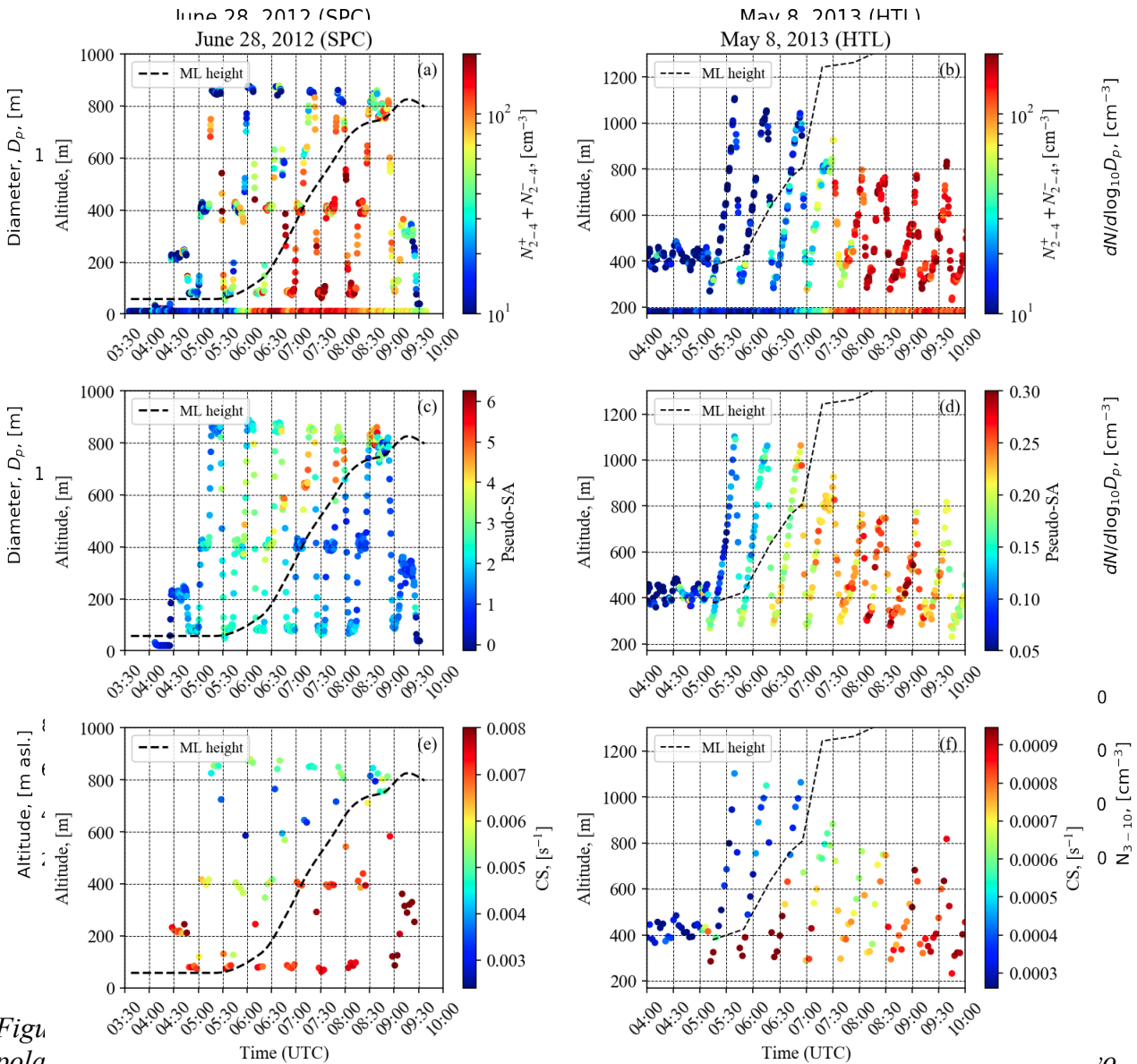


Figure 6

The black dots are the mean mode diameters found by fitting a log-normal

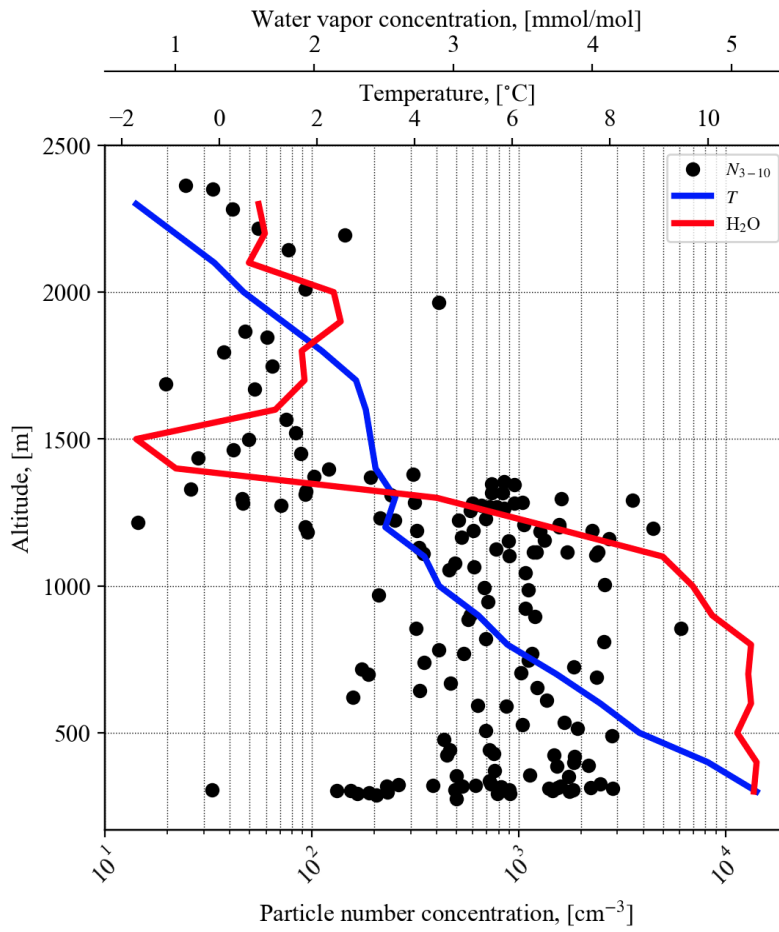


Figure 7: Vertical profile of 3-10 nm particle number concentration (black dots), temperature (blue line) and water vapor concentration (red line) measured on board the Cessna between 07:00-10:00 on May 8, 2013 in HTL.

729 Figure 6. Time evolution of particle number size distributions measured by the NAIS (positive
 730 polarity) on board the Zeppelin (a, b) and at the ground level (c, d) in HTL and in SPC on the two
 731 case study days. The black dots are the mean mode diameters found by fitting a log-normal
 732 distribution over the growing mode.

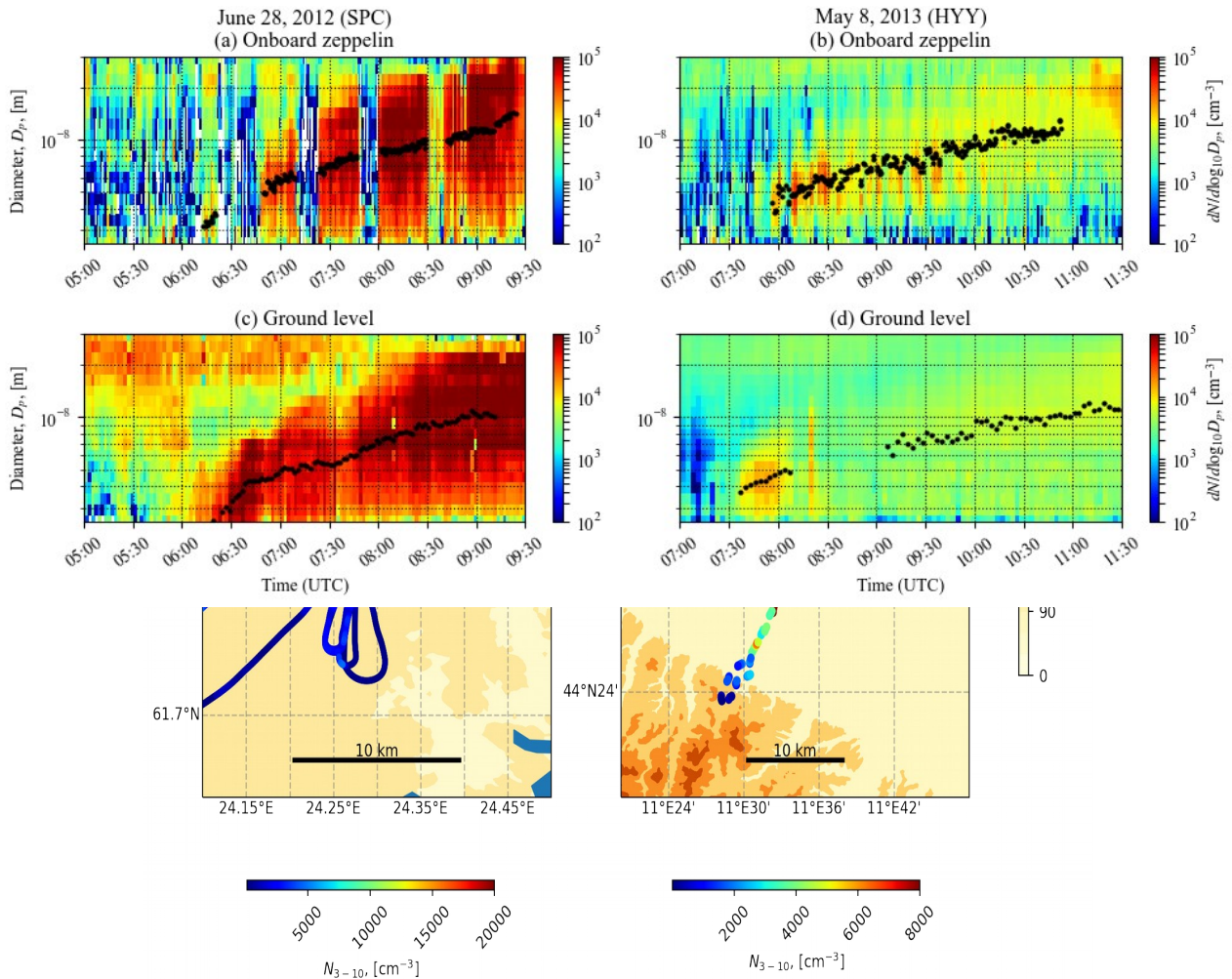
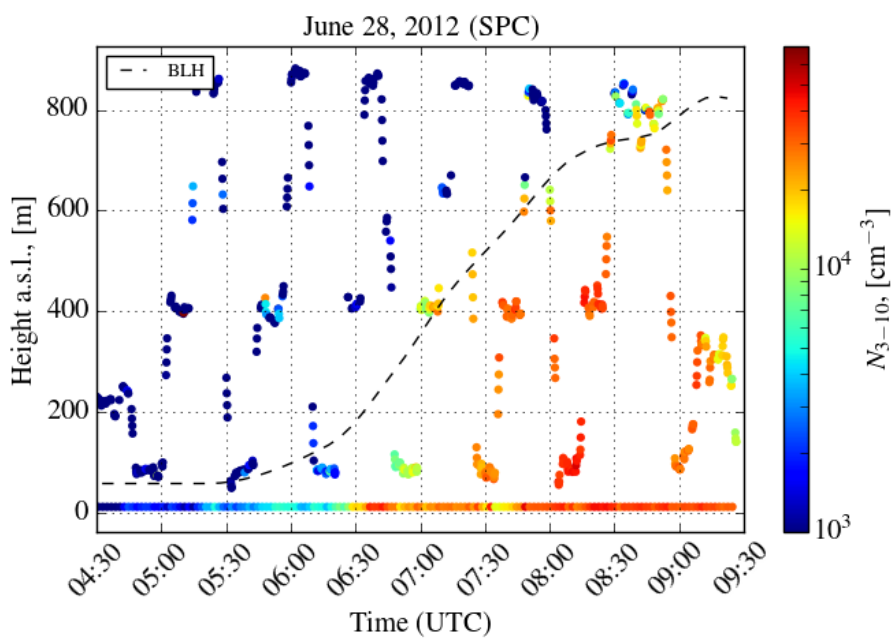
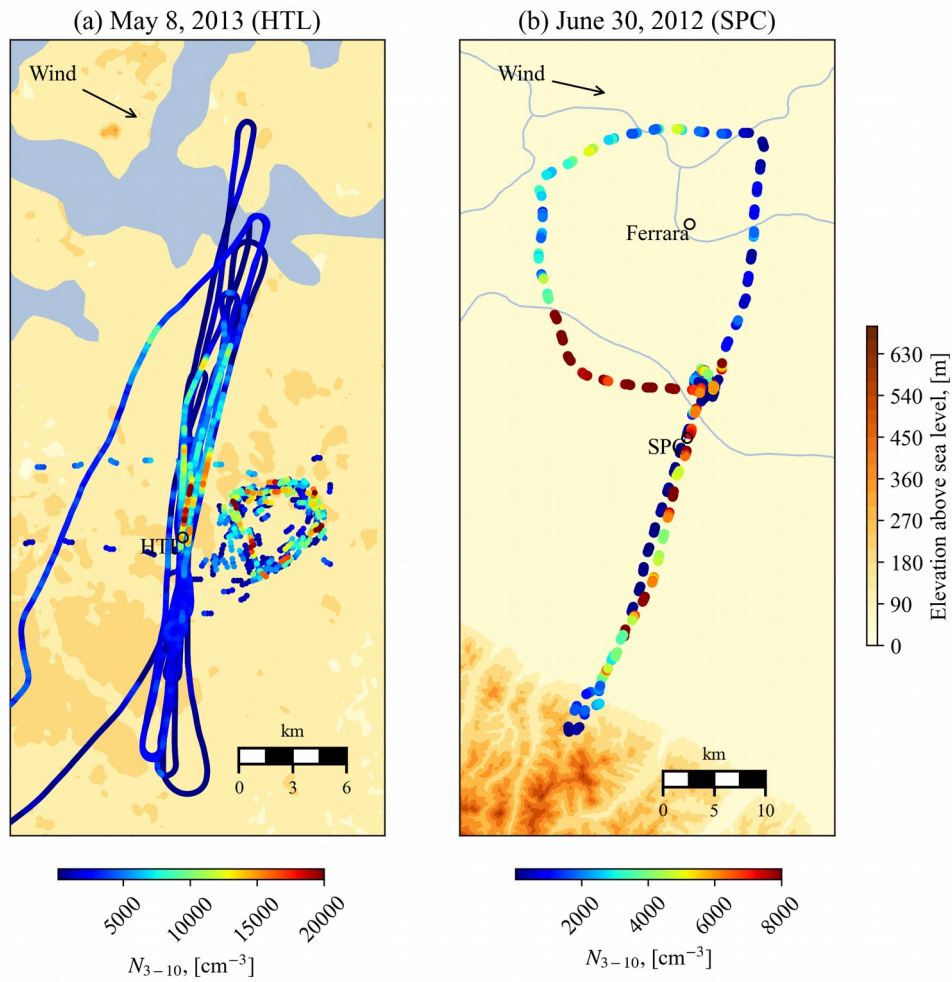


Figure 8: (a) the flight tracks of the Zeppelin (circular track) and the airplane (track with back an forth segments) colored by 3-10 nm particle number concentration from HTL on May 8, 2013. (b) the flight track of the Zeppelin colored by 3-10 nm particle number concentration from SPC on June 30, 2012. The Zeppelin flight track has gaps because the NAIS was measuring in the ion mode during that time.

734 | Figure 7. The particle number concentration in the 3-10 nm size range from SPC on board the
735 | Zeppelin and on the ground level on June 28, 2012. BLH refers to the boundary layer height
736 | determined from ceilometer.



738 | ~~Figure 8: Vertical profile of 3-10 nm particle number concentration (black dots), temperature (blue~~
739 | ~~line) and water vapor concentration (red line) measured on board the Cessna between 07:00-10:00~~
740 | ~~on May 8, 2013 in HTL.~~



741 Figure 9: (a) the flight tracks of the Zeppelin (circular track) and the airplane (track with back an-
 742 forth segments) colored by 3-10 nm particle number concentration from HTL on May 8, 2013. (b)-
 743 the flight track of the Zeppelin colored by 3-10 nm particle number concentration from SPC on June
 744 30, 2012. The Zeppelin flight track has gaps because the NAIS was measuring in the ion mode-
 745 during that time.

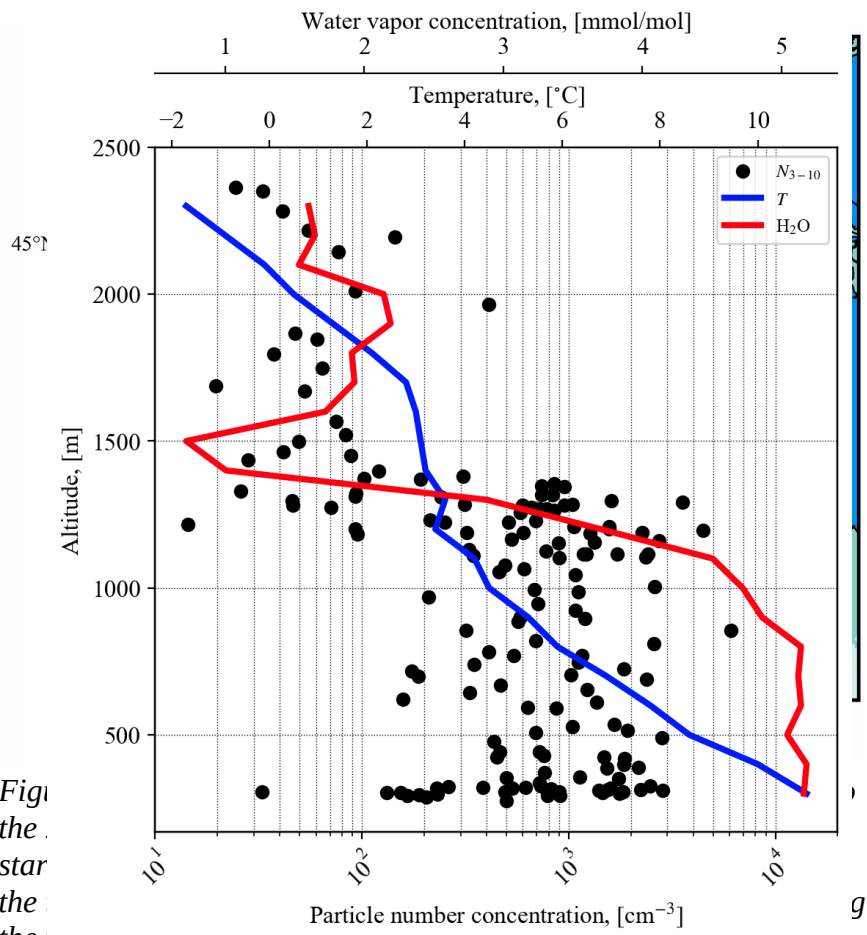


Fig. 1. The trajectory of the star is shown. The red line is the Zeppelin's flight track.

747 | Figure 10: Airmass back trajectories (black dotted lines) arriving to the Zeppelin's measurement
748 | area over north Italy on June 30, 2012. The separation between the dots along the trajectories is one
749 | hour. The red line is the Zeppelin's flight track.

750 | ~~Table 1. Calculated particle formation and growth rates. + and - superscripts refer to positive and~~
751 | ~~negative ions respectively. The Zeppelin missed the beginning of the NPF event in SPC and because~~
752 | ~~of that some values are missing.~~

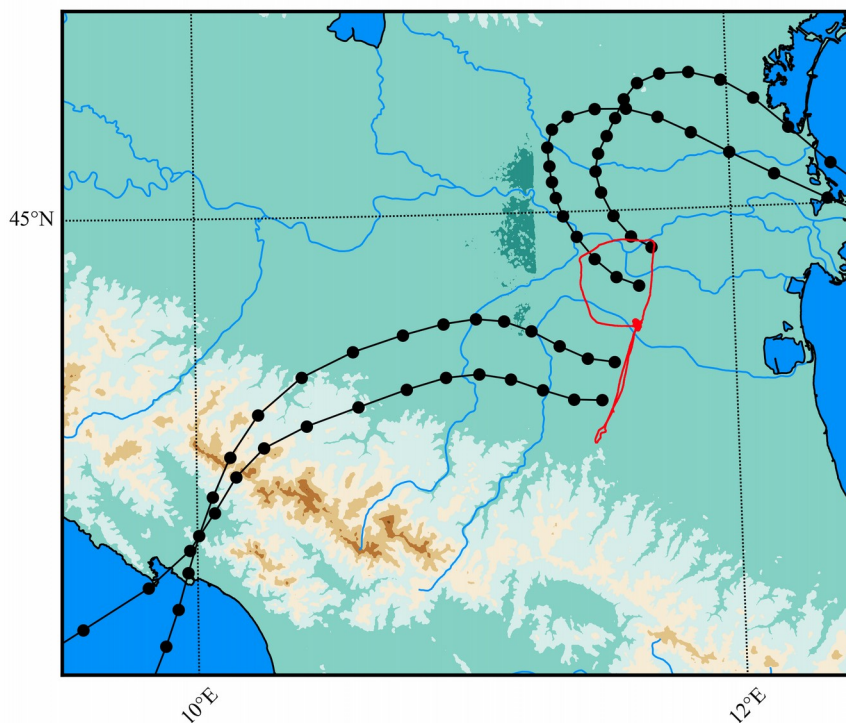


Table 1: Calculated particle formation and growth rates. + and – superscripts refer to positive and negative ions respectively. The Zeppelin missed the beginning of the NPF event in SPC and because of that some values are missing.

	HTL (May 8, 2013)		SPC (June 28, 2012)	
	Zeppelin	Ground	Zeppelin	Ground
$J_{1.5}$, [$\text{cm}^{-3} \text{s}^{-1}$]	1.5	0.9	-	-
J_3 , [$\text{cm}^{-3} \text{s}^{-1}$]	0.2	0.3	-	6.8
J_3^- , [$\text{cm}^{-3} \text{s}^{-1}$]	0.04	0.04	-	0.04
J_3^+ , [$\text{cm}^{-3} \text{s}^{-1}$]	0.04	0.04	-	0.03
GR_{1-2} , [nm h^{-1}]	0.8	0.7	-	0.5
GR_{2-3} , [nm h^{-1}]	1.4	1.5	1.8	1.5
GR_{3-7} , [nm h^{-1}]	1.7	1.6	2.9	2.0
GR_{7-20} , [nm h^{-1}]	2.4	2.1	3.0	2.8